

Higgs funnel region of SUSY dark matter for small $\tan\beta$, RG effects on pseudoscalar Higgs boson with scalar mass non-universality

Utpal Chattopadhyay and Debottam Das¹

*Department of Theoretical Physics
Indian Association for the Cultivation of Science
2A and 2B Raja S.C. Mullick Road
Jadavpur, Kolkata 700 032, India*

Abstract

A non-universal scalar mass supergravity type of model is explored where the first two generation of scalars and the third generation of sleptons may be very massive. Lighter or vanishing third generation of squarks as well as Higgs scalars at the unification scale cause the radiative electroweak symmetry breaking constraint to be less prohibitive. Thus, both FCNC/CP-violation problems as well as the naturalness problem are within control. We identify a large slepton mass effect in the RGE of $m_{H_D}^2$ (for the down type of Higgs) that may turn the later negative at the electroweak scale even for a small $\tan\beta$. A hyperbolic branch/focus point like effect is found for m_A^2 that may result in very light Higgs spectra. The lightest stable particle is dominantly a bino that pair annihilates via Higgs exchange, giving rise to a WMAP satisfied relic density region for all $\tan\beta$. Detection prospects of such LSPs in the upcoming dark matter experiments both of direct and indirect types (photon flux) are interesting. The Higgs bosons and the third generation of squarks are light in this scenario and these may be easily probed besides charginos and neutralinos in the early runs of LHC.

1 Introduction

Low energy supersymmetry (SUSY) [1] is one of the most active field of research for physics beyond the standard model (SM) [2]. A minimal extension of the standard model when supersymmetry is incorporated is the Minimal Supersymmetric Standard Model (MSSM)

¹Emails: tpuc@iacs.res.in, tpdd@iacs.res.in

[1, 3] that includes two Higgs doublets. The model however has a large number of SUSY breaking parameters and this motivates one into studying models with specific mechanisms for breaking SUSY. This involves high scale physics input and renormalization group analyses leading to a large reduction of the number of unknown parameters. The minimal supergravity (mSUGRA) [4] model is one of the well studied SUSY models. It requires a very few input parameters at the gauge coupling unification scale or grand unified theory (GUT) scale, $M_G \simeq 2 \times 10^{16}$ GeV. The parameters indeed quantify our ignorance of the exact nature of the supersymmetry breaking. The model incorporates radiative breaking of electroweak symmetry (REWSB). The unification scale universal input parameters are: i) the gaugino mass parameter $m_{\frac{1}{2}}$, ii) the scalar mass parameter m_0 and iii) the tri-linear SUSY breaking parameter A_0 . Additionally, one has to provide with $\tan\beta$, the ratio of Higgs vacuum expectation values and the sign of the Higgsino mixing parameter μ . Renormalization group evolutions are used to obtain the electroweak scale parameters of MSSM.

There is however no *a priori* necessity of considering such universalities of parameters. Indeed it is worthwhile to explore scenarios with non-universalities in the scalar or the gaugino masses at the unification scale [5–11]. Non-universal scalar masses may appear because of non-flat Kähler potential [12]. However, one must be careful to accommodate the stringent constraints from phenomena involving flavor changing neutral currents (FCNC). Satisfying FCNC constraints demands near-degeneracy of the first two generations of scalar masses but the requirements on the third generation of scalars as well as the Higgs scalars are not so stringent [13, 14]. Thus it is seen that FCNC constraints as well as constraints from CP-violating phases (for example from the electric dipole moments of electron and neutron) can be managed by introducing multi-TeV scalar masses for the first two generations of scalars [15]. The third generations of scalar masses and Higgs scalar masses however should be adequately light in order to satisfy naturalness [16]. There have been several efforts for obtaining the desired features as outlined above. An analysis with Radiatively Generated Inverted Mass Hierarchy Models (RIMH) was made in Ref. [14, 17, 18]. In Ref. [18] the authors achieved the above requirements at the electroweak scale by using $t - b - \tau$ Yukawa unification with special non-universal relationship among the scalar masses at M_G . Here, the Higgs and the third generation of scalar masses are rapidly diminished by RG evolutions toward the electroweak scale. However, the Yukawa unification and the consideration of REWSB highly constrain such models. A second realization of the above idea is partially

possible via the hyperbolic branch (HB)/ Focus Point (FP) [19,20] scenarios where the scalars may become considerably massive (multi-TeV) in a subset of the typical mSUGRA parameter space satisfying universal boundary conditions while fine-tuning [16] still remaining small. A third possibility was considered in Ref. [21], where plain decoupling arguments motivated the authors in using explicit splitting between the scalars belonging to the first two generations and the same of the third generation (along with the Higgs scalars) and this was introduced at the GUT scale itself. Here the first two generations of scalars are chosen in the multi-TeV domain whereas the the third generation of scalars as well as the Higgs scalars stay in the sub-TeV zone. Additionally, a large value of tri-linear coupling parameter was chosen in Ref. [21] for the first two-generations. Universality of scalar masses in the first two-generations with a choice of a different scalar mass for the third generation as well as the Higgs, or even splitting of squarks and sleptons within the third generation itself have also recently been considered in Refs. [22–24]. In Ref. [23] the authors additionally considered non-universality in the gaugino masses and analyzed the fine-tuning aspect of computing the relic density of dark matter. The authors investigated the possibility of obtaining a parameter zone of MSSM corresponding to a well tempered neutralino [25]. Similarly, non-universal Higgs scalar analyses may be seen in Refs. [6, 8, 10, 26]. A comprehensive set of characteristic possibilities for varieties of non-universal SUGRA scenarios may be seen in Ref. [27].

In this analysis we explore a SUGRA scenario with non-universal scalar masses that i) allows to have large first two-generation of scalar masses so as to obey the FCNC and the CP-violation limits easily (*ie.* without requiring any ultra-small phases) and that would not impose any additional price on fine-tuning, ii) spans a large amount of MSSM parameter space satisfying the neutralino relic density constraint from WMAP data by not having any delicate mixing of bino and Higgsinos, so that we would find a bino-dominated lightest neutralino for most of the parameter space and, iii) satisfies the Higgs mass lower bound from LEP2 data as well as other low energy constraints. Certainly, a model with REWSB and universal scalar mass like mSUGRA is not friendly to achieve these objectives if we consider a common gaugino mass parameter below a TeV or so. The above phenomenologically inspired requirements in combination motivate us to introduce non-universality between the third and the first two-generation of scalars as well as the Higgs scalars. This has to be such that the REWSB conditions would not become prohibitive to have a multi-TeV first

two-generation of scalars. Here we would like to point out that using only non-universal values for the Higgs scalar mass parameters and keeping all other scalar mass parameters common at the unification scale would not achieve the above purpose.

A simpler and a purely phenomenological attempt in this direction in a universal gaugino mass framework could be to try to generate all the third generation of scalar masses and the Higgs scalar masses radiatively, starting from zero values at the unification scale, while keeping the first two-generations of scalar masses to be universal (and this may be in the multi-TeV zone). We point out that starting with similar range of values for the Higgs scalars as with the third generation of scalars at M_G would be desirable since this would lead to similar range of mass values for all the soft-SUSY breaking terms contributing to REWSB after RG evolutions. However, if we consider all the third generation of scalars at M_G to be light, we would find stau ($\tilde{\tau}$) becoming the lightest stable particle (LSP) or even tachyonic at the electroweak scale. On a similar note, we remind that such appearance of tachyonic sleptons also arise in the Anomaly Mediated Supersymmetry Breaking (AMSB) analyses, and it is avoided purely by a phenomenologically inspired way of adding an appropriate non-zero mass value to all the scalars at the unification scale in the minimal AMSB scenario [28]. Thus with a simple motivation of concurrently managing with FCNC and CP-violation, naturalness as well as the dark matter constraints we consider a non-zero mass value for the third generation of sleptons, while fixing the squarks of the third generation and the Higgs scalars to have vanishing masses at M_G . Additionally, for convenience we set the third generation of slepton mass parameters same as that of the first two-generation of scalars at M_G .

Thus, the parameters of our Non-universal Scalar Mass model which will henceforth be called NUSM model is given by

$$\tan \beta, m_{\frac{1}{2}}, A_0, \text{sign}(\mu), \text{ and } m_0 \tag{1}$$

where the scalar mass input assignments at M_G are as follows.

- i) The unification scale mass parameter for the first two-generation of squarks, sleptons and third generation of sleptons is m_0 , where m_0 is allowed to vary up to a very large value.
- ii) The same for the third generation of squarks and Higgs scalars are set to zero.

We could have also chosen a different value than zero for ii) as long as it is sufficiently small. We may note here that different values of mass parameters for squarks and sleptons at M_G may appear in orbifold models with large threshold corrections. This is related to

having different modular weights associated with the squarks and the sleptons in a given generation [29, 30].

As we will see below, the NUSM model provides with a highly bino-dominated neutralino dark matter over almost its full range of parameter space and it has an interesting feature of producing a large funnel region *i.e.* the annihilation channels are characterized by the direct channel pole $2m_{\tilde{\chi}_1^0} \simeq m_A, m_H$. We note that unlike mSUGRA where one finds the funnel region only for a large $\tan\beta$, here one finds it for all possible values of $\tan\beta (\gtrsim 5)$. We will also see that NUSM is further characterized by a lighter m_A or m_H as m_0 increases and this happens even for small values of $\tan\beta (\gtrsim 10)$. A small part of the parameter space may be far from the decoupling [31] region of Higgs boson mixing that causes the lighter CP-even Higgs boson (h -boson) to be non-Standard Model like [32]. This in turn reduces the lower bound of m_h much below the LEP2 Higgs boson mass limit.

In this work we include a semi-analytic calculation that first points out a large mass effect in the solution of the renormalization group equations (RGE) of $m_{H_D}^2$. The effect causes a hyperbolic branch/focus point like behavior² in $m_A^2 (\simeq m_{H_D}^2 - m_{H_U}^2)$ that may cause m_A to become smaller even for a small $\tan\beta$. Here we remind that m_A typically becomes smaller in mSUGRA only for large $\tan\beta$.

The paper is organized as follows. In Sec.2 we will primarily discuss the large mass RGE effects of the non-universal scalar mass scenario (NUSM) on m_A^2 and its consequent reduction via a HB/FP-like effect by showing semi-analytic results as well as numerical verifications. In Sec.3 we will study the cold dark matter constraint from WMAP data including also the constraints from LEP2 Higgs bound, $b \rightarrow s + \gamma$, and $B_s \rightarrow \mu^+ \mu^-$. We will also discuss a few sample points in the context of LHC reach. In Sec.4 we will discuss the direct and indirect detection (via continuous gamma ray) rates of LSP. Finally we will conclude in Sec.5.

2 The non-universal scalar scenario:NUSM

In this section we focus on the key elements that are important for NUSM. The primary quantities of phenomenological interest which have dominant effects because of considering

²We remind that the well known HB/FP effect that occurs in $m_{H_U}^2$ is associated with the first minimization condition of Radiative electroweak symmetry breaking. In this analysis we do not have such an effect. On the contrary we have a similar HB/FP effect for small values of $\tan\beta$ in connection with the second minimization condition that is associated with m_A^2 .

the above non-universality are μ , and m_A . These in turn have important significance on the following: i) the issue of fine-tuning, ii) presence of non-Standard Model like lighter Higgs boson mass bound for a limited region of parameter space, iii) dark matter and iv) collider discovery possibilities. Additionally we remind ourselves about obtaining a lighter third generation of squarks at the electroweak scale and this is of course related to their vanishing values at the unification scale.

To start with we write down the REWSB results,

$$\mu^2 = -\frac{1}{2}M_Z^2 + \frac{m_{H_D}^2 - m_{H_U}^2 \tan^2 \beta}{\tan^2 \beta - 1} + \frac{\Sigma_1 - \Sigma_2 \tan^2 \beta}{\tan^2 \beta - 1}, \quad (2)$$

and,

$$\sin 2\beta = 2B\mu / (m_{H_D}^2 + m_{H_U}^2 + 2\mu^2 + \Sigma_1 + \Sigma_2) \quad (3)$$

where Σ_i represent the one-loop corrections [33, 34], that become small in the scale where the Higgs potential V_{Higgs} is minimized. We may approximately consider $\mu^2 \simeq -m_{H_U}^2$ (for $\tan \beta \gtrsim 5$) and $m_A^2 = m_{H_D}^2 + m_{H_U}^2 + 2\mu^2 \simeq m_{H_D}^2 - m_{H_U}^2$ at tree level.

The associated one-loop RGEs are given by (neglecting the very small first two-generation of Yukawa contributions),

$$\begin{aligned} \frac{dm_{H_D}^2}{dt} &= (3\tilde{\alpha}_2 \tilde{m}_2^2 + \frac{3}{5}\tilde{\alpha}_1 \tilde{m}_1^2) - 3Y_b(m_{H_D}^2 + m_Q^2 + m_D^2 + A_b^2) \\ &\quad - Y_\tau(m_{H_D}^2 + m_L^2 + m_E^2 + A_\tau^2) + \frac{3}{10}\tilde{\alpha}_1 S_0 \end{aligned} \quad (4)$$

$$\frac{dm_{H_U}^2}{dt} = (3\tilde{\alpha}_2 \tilde{m}_2^2 + \frac{3}{5}\tilde{\alpha}_1 \tilde{m}_1^2) - 3Y_t(m_{H_U}^2 + m_Q^2 + m_U^2 + A_t^2) - \frac{3}{10}\tilde{\alpha}_1 S_0 \quad (5)$$

Here $t = \ln(M_G^2/Q^2)$ with Q being the renormalization scale. $\tilde{\alpha}_i = \alpha_i/(4\pi)$ for $i = 1, 2, 3$ are the scaled gauge coupling constants (with $\alpha_1 = \frac{5}{3}\alpha_Y$) and \tilde{m}_i are the running gaugino masses. Y_i represents the scaled and squared Yukawa couplings, e.g, $Y_i \equiv h_i^2/(4\pi)^2$ where h_i is a Yukawa coupling. The quantity S_0 which is shown below may become relevant for a general set of non-universal boundary condition for scalars. However in this analysis it is zero at M_G to cause only a negligible effect.

$$S_0 = m_{H_U}^2 - m_{H_D}^2 + \Sigma_i(m_{q_i}^2 + m_{d_i}^2 + m_{e_i}^2 + m_{l_i}^2 - 2m_{\tilde{u}_i}^2) + (m_Q^2 + m_D^2 + m_E^2 - m_L^2 - 2m_U^2) \quad (6)$$

where the subscript i for $i=1$ or 2 indicates the first two-generations.

μ^2 and m_A^2 are evaluated at the one-loop level of the effective potential when the minimization of V_{Higgs} is performed at a scale where Σ_i 's are small [20]. Typically the solutions for μ^2 and m_A^2 up to a moderately large value of $\tan \beta$ (10 or so) follows from Ref. [6] after appropriately considering the NUSM parameters. This involves ignoring h_b and h_τ in the limit of a small $\tan \beta$. However, we will see that the solution is in no way complete to describe the large mass effect.

$$\mu^2 = m_0^2 C_1 + A_0^2 C_2 + m_{\frac{1}{2}}^2 C_3 + m_{\frac{1}{2}} A_0 C_4 - \frac{1}{2} M_Z^2 + \frac{3 \tan^2 \beta + 1}{5 \tan^2 \beta - 1} S_0 p \quad (7)$$

$$m_A^2 = m_0^2 D_1 + A_0^2 D_2 + m_{\frac{1}{2}}^2 D_3 + m_{\frac{1}{2}} A_0 D_4 - \frac{1}{2} M_Z^2 + \frac{6 \tan^2 \beta + 1}{5 \tan^2 \beta - 1} S_0 p \quad (8)$$

Here only C_1 among C_i 's and D_1 among D_i 's depend on δ and one obtains³,

$$\begin{aligned} C_1 &= (1 + \delta) \frac{1}{\tan^2 \beta - 1} \left(1 - \frac{3D_0 - 1}{2} \tan^2 \beta\right) \\ D_1 &= \frac{3}{2} (1 + \delta) \frac{\tan^2 \beta + 1}{\tan^2 \beta - 1} (1 - D_0) \end{aligned} \quad (9)$$

The definitions of the quantities C_i and D_i for $i \neq 1$ may be seen in the Appendix. For NUSM one has $\delta = -1$. Hence, Eqns. 7-9 show that at this level of approximation of ignoring h_b and h_τ , μ^2 and m_A^2 are independent of m_0 . We will however see that both μ^2 and m_A^2 would actually depend on m_0 . While the dependence of μ^2 on m_0 would be caused by two-loop RGE effects in $m_{H_U}^2$, the same for m_A^2 is very prominent even at the one-loop level of RGE. The following subsection describes the effect.

2.1 Large slepton mass RGE effect on pseudoscalar Higgs boson— A hyperbolic branch/focus point like effect in m_A^2 for small $\tan \beta$

Numerical computation shows that unlike Eqns. 8 and 9, m_A^2 may indeed decrease very rapidly with m_0 for large values of the later. There are two reasons behind the above behavior: i) choice of vanishing Higgs scalars in NUSM at the unification scale M_G and ii) a

³In Ref. [6] the authors considered non-universalities in the masses of Higgs scalars and the third generation scalars m_{Q_L} and m_{u_R} . However, NUSM additionally requires non-universality in m_{d_R} .

large slepton mass (LSM) effect in the RGE of Eq.4 via the tau-Yukawa term. Henceforth, we will refer the combined effect of i) and ii) as LSM effect. In this analysis we first compute $m_{H_D}^2$ analytically without ignoring the terms involving h_b and h_τ . The calculation essentially keeps the terms involving the bottom and the tau-Yukawa couplings similar to what was used for the top-Yukawa term of Eq.4 in Refs. [6, 35]. This results into,

$$m_{H_d}^2 = C_{H_D} m_0^2 + m_{1/2}^2 g(t) + \frac{3}{5} S_0 p. \quad (10)$$

Here $g(t)$ is a function of $\tan \beta$ [35] and $p = \frac{5}{66} [1 - (\frac{\tilde{\alpha}_1(t)}{\tilde{\alpha}_1(0)})]$. The term involving S_0 vanishes in NUSM. At the level of approximation where the bottom and tau Yukawa couplings are straightway ignored in Eq.4, C_{H_D} would be zero in NUSM. The result of our computation of C_{H_D} that provides a non-vanishing value is given below.

$$C_{H_D} = C_{H_D}(U) + C_{H_D}(NU) \quad (11)$$

where,

$$\begin{aligned} C_{H_D}(U) &= 1 - 3(3I_2 + I_3) \\ C_{H_D}(NU) &= \delta_{H_D} - 3I_2(\delta_{Q_L} + \delta_{d_R} + \delta_{H_D}) \\ &\quad - I_3(\delta_{l_L} + \delta_{e_R} + \delta_{H_D}) \end{aligned} \quad (12)$$

Here, the quantities δ_i where $i \equiv H_D, H_U, Q_L, u_R, d_R, l_L, e_R$ are given by $m_i^2 = (1 + \delta_i)m_0^2$. For NUSM one has $\delta_{H_u} = \delta_{H_D} = \delta_{Q_L} = \delta_{u_R} = \delta_{d_R} = -1$ and $\delta_{l_L} = \delta_{e_R} = 0$. The quantities I_2 and I_3 are functions of $Y_i = \frac{h_i^2}{(4\pi)^2}$ for $i = 2, 3$ (b, τ). Small $\tan \beta$ solutions of Y_i s, computed at the electroweak scale [35] are shown in the Appendix. I_2 and I_3 defined below are computed numerically.

$$I_2 = \int_0^t Y_2(t') dt', \quad I_3 = \int_0^t Y_3(t') dt' \quad (13)$$

Here $t = \ln(M_G^2/M_Z^2)$. One finds $I_2, I_3 \ll 1$. For NUSM, the above reduces to

$$C_{H_D} = -2I_3. \quad (14)$$

For $\tan \beta = 10$, we find $C_{H_D} \simeq -0.007$. The above clearly shows the large slepton mass effect because I_3 corresponds to the h_τ -dependent term in Eq.4. Thus with NUSM parameters, the scalar mass term that appears as the first term in Eq.10 is essentially contributed by the third generation of slepton masses. Eq.10 and Eq.14 clearly show that even with a small

$\tan \beta$, larger values of m_0 may reduce $m_{H_D}^2$ appreciably and may turn the later negative. This demonstrates the LSM effect as mentioned before. We are not aware of any past reference that pointed out this large mass effect or provided with semi-analytic expressions. For larger $\tan \beta$, C_{H_D} may be appreciably large and negative that causes the LSM effect to become prominent even for a smaller value of m_0 .

We note that there is no LSM effect that may modify μ^2 of Eq.7 at one-loop level. This is simply because with $m_{H_U}^2 \simeq -\mu^2$ and with $\delta = -1$ for NUSM (see Eq.9), $m_{H_U}^2$ does not have any dependence on m_0 . On the other hand, an improved $m_{H_D}^2$ as obtained above in Eqs.10 and 14 changes the result of m_A^2 (Eq.8 and 9) but the later does not receive any additional m_0^2 dependent term other than what is already there via Eq.14. Thus it follows that the coefficient of m_0^2 when Eq.8 is modified would be C_{H_D} . As a result, in the above analysis that is valid for small $\tan \beta$, we find that the LSM effect causes a HB/FP like behavior in m_A^2 for its dependence on m_0 and $m_{\frac{1}{2}}$. Hence, m_A may become significantly small for a large m_0 because of cancellation between the terms and this happens even for a small value of $\tan \beta$. A very large m_0 would cause m_A^2 to become tachyonic, or breakdown of REWSB (Eq.3). For a large $\tan \beta$ on the other hand, the effect is drastically enhanced. We comment here that in spite of showing the one-loop results we performed a complete numerical solution of the RGEs up to two loops in this analysis using SUSPECT [36].

We now point out that a simple non-universal Higgs scalar mass scenario as described in Ref. [10] may also provide with a small m_A along with a funnel type of region that satisfies the WMAP data, for a smaller value of $\tan \beta$. We emphasize in particular the case where non-universality was analyzed with a unified Higgs scalar mass in Ref. [10]. However, unlike NUSM these scenarios are very much constrained via REWSB so that considering larger values of masses for the first two-generation of scalars, an easier way to control FCNC and CP-violation effects is not possible. In these non-universal Higgs scalar models m_A becomes small for small values of $\tan \beta$ only when tachyonic values of $m_{H_D}^2$ and $m_{H_U}^2$ (assumed equal) are considered at the unification scale and this severely reduces the available parameter space. Additionally, one may obtain an A -pole annihilation region or a funnel region for a small value of $\tan \beta$ in the so called sub-GUT CMSSM scenario [37].

We will now describe our results as obtained by using SUSPECT [36]. Fig.1 shows the variation of μ and m_A when m_0 is varied in NUSM and mSUGRA. Fig.1(a) shows the effect of varying m_0 in mSUGRA and in NUSM for $m_{1/2} = 500$ GeV and 1 TeV. A small

reduction of $|\mu|$ ((10 to 20%)) is seen in NUSM when m_0 is increased up to 5 or 10 TeV. The approximate one-loop result of Eq.7 and Eq.9 with $\delta = -1$ as in NUSM however would indicate a flat μ over a variation of m_0 . The figure of course shows a moderately varying μ and we have checked that this variation has its origin in two-loop RGE effects. The two different $m_{1/2}$ contours for mSUGRA however show a decreasing behavior of μ when m_0 is enhanced. This happens simply because of the HB/FP effect existing in mSUGRA. Fig.1(b) shows the results for m_A which has two sets of contours for $m_{1/2} = 500$ GeV and 1 TeV corresponding to mSUGRA and NUSM. In contrast to mSUGRA where m_A rapidly increases with m_0 , the behavior in NUSM is opposite so that we may find a very light pseudoscalar Higgs boson via the LSM effect. The decrease of m_A is even more pronounced for a large value of $\tan\beta$ and this may be easily seen in Fig.1(c) where a variation of m_A vs m_0 is shown for a given $m_{1/2}(= 500$ GeV) for three different values of $\tan\beta$. The curves ends in the larger m_0 sides for a few different reasons. For $\tan\beta \lesssim 10$, the largest m_0 limit is caused by stop mass becoming very light or unphysical. On the other hand for $\tan\beta \gtrsim 15$ the largest m_0 limit is given by absence of REWSB (ie m_A^2 turning negative).

The LSM effect may be explicitly seen in Fig.2 where we plot squared scalar masses of Higgs scalars as well as their difference $m_A^2 \simeq m_{H_D}^2 - m_{H_U}^2$ with respect to a variation over the renormalization scale Q for mSUGRA and NUSM for $\tan\beta = 10$ and $m_{1/2} = 400$ GeV and $A_0 = 0$. Fig.2(a) corresponds to mSUGRA for $m_0 = 1$ TeV whereas Fig.2(b) shows the case of NUSM for $m_0 = 5$ TeV. We have chosen different values of m_0 in the two figures because of the fact that a large m_0 is prohibited in mSUGRA via the REWSB constraint whereas a choice of a small m_0 in NUSM would not demonstrate the LSM effect prominently. Clearly, $m_{H_D}^2$ stays positive at the electroweak scale in mSUGRA (Fig.2(a)). On the other hand the same for NUSM turns toward a negative value while running from M_G to the electroweak scale (Fig.2(b)) and this essentially shows the LSM effect in m_A^2 . Thus a typical large $\tan\beta$ phenomenon that occurs in mSUGRA is obtained in NUSM for a small $\tan\beta$.

3 Cold dark matter constraint and extended funnel region

In supergravity type of models $\tilde{\chi}_1^0$ becomes the LSP for most of the parameter space [38, 39] and we assume that the cold dark matter relic density is entirely due to $\tilde{\chi}_1^0$. Considering

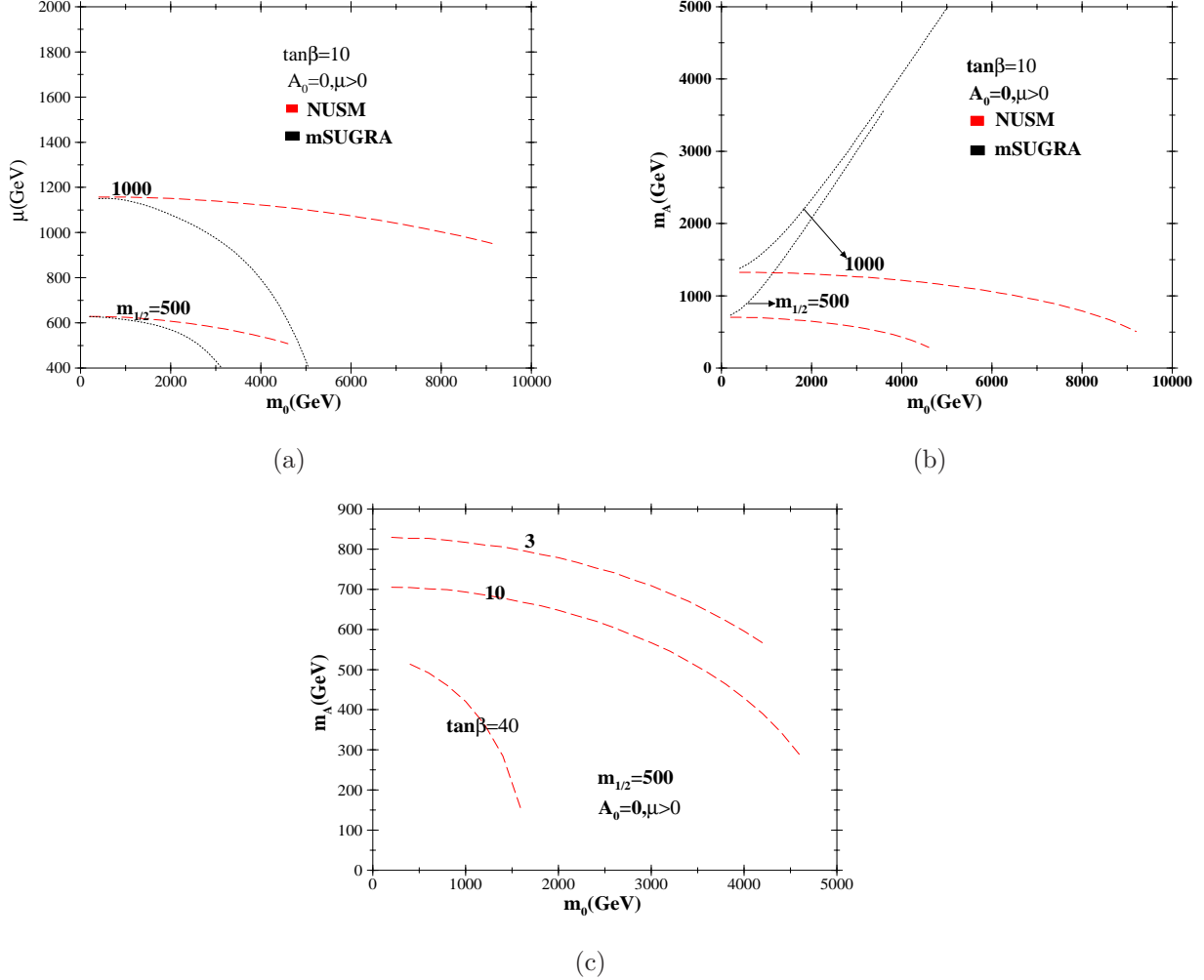


Figure 1: (a) Variation of μ with m_0 for $\tan\beta = 10$, $A_0 = 0$ and $m_{\frac{1}{2}} = 500, 1000\text{GeV}$. The red dashed lines represent the curves for NUSM and the black dotted lines represent the same for mSUGRA. (b) same as (a), but CP-odd Higgs(m_A) is plotted against m_0 . (c) shows the variation of m_A with m_0 in NUSM for different values of $\tan\beta$ when $m_{\frac{1}{2}} = 500\text{GeV}$.

WMAP data [40] one finds a 3σ limit as shown below.

$$0.091 < \Omega_{CDM} h^2 < 0.128 \quad (15)$$

where $\Omega_{CDM} h^2$ is the DM relic density in units of the critical density. Here, $h = 0.71 \pm 0.026$ is the Hubble constant in units of $100 \text{ Km s}^{-1} \text{ Mpc}^{-1}$. In the thermal description, the LSP was in thermal equilibrium with the annihilation products at a very high temperature of the early universe ($T \gg m_{\tilde{\chi}_1^0}$). The annihilation products include fermion pairs, gauge boson

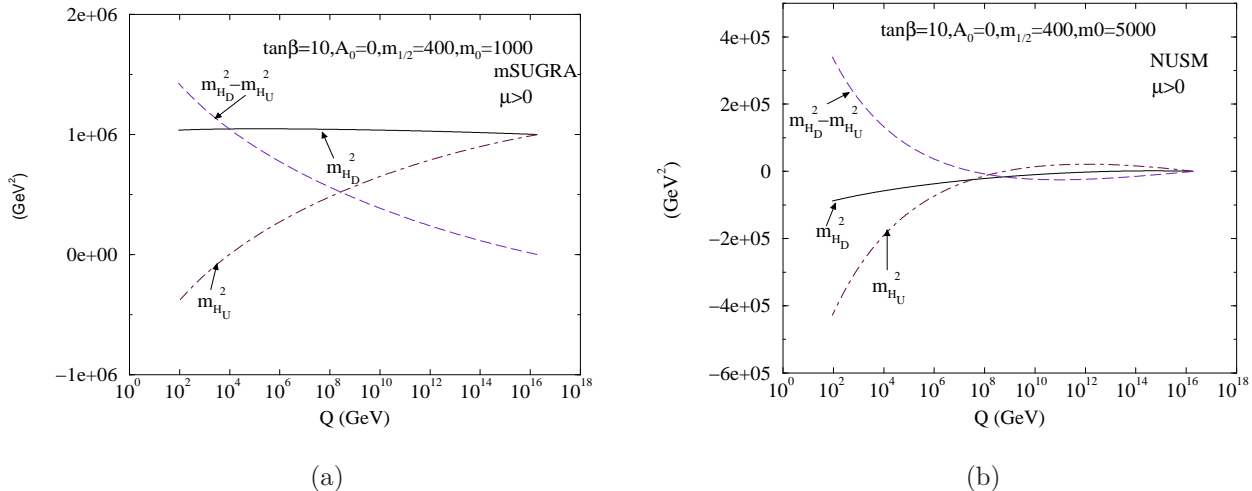


Figure 2: (a) Variation of squared Higgs scalar masses and their difference ($\equiv m_A^2 \simeq m_{H_D}^2 - m_{H_U}^2$) with renormalization scale Q for $\tan\beta = 10$, $m_{\frac{1}{2}} = 400$ GeV, $m_0 = 1000$ GeV and $A_0 = 0$ for mSUGRA. (b) same as (a), except for $m_0 = 5000$ GeV and for NUSM. $m_{H_D}^2$ turns negative via LSM effect.

pairs, Higgs boson pairs or gauge boson-Higgs boson combinations and they are produced via s, t and u -channel processes. As temperature decreased the annihilation rate fell below the expansion rate of the universe and the LSP went away from the thermal equilibrium and freeze-out occurred. The current value of $\Omega_{\tilde{\chi}_1^0} h^2$ is computed by solving the Boltzmann equation for $n_{\tilde{\chi}_1^0}$, the number density of the LSP in a Friedmann-Robertson-Walker universe. The above computation essentially involves finding the thermally averaged quantity $\langle \sigma_{eff} v \rangle$, where v is the relative velocity between two annihilating neutralinos and σ_{eff} is the neutralino annihilation cross section that includes all the final states. In addition to annihilations one considers coannihilations [41–45] which are annihilations of the LSP with sparticles close in mass values with that of the LSP. The cross section sensitively depends on the nature of the composition of the LSP. In MSSM, LSP is a mixed state of bino (\tilde{B}), wino (\tilde{W}) and Higgsinos ($\tilde{H}_1^0, \tilde{H}_2^0$):

$$\tilde{\chi}_1^0 = N_{11}\tilde{B} + N_{12}\tilde{W}_3 + N_{13}\tilde{H}_1^0 + N_{14}\tilde{H}_2^0. \quad (16)$$

Here N_{ij} are the elements of the matrix that diagonalizes the neutralino mass matrix. The gaugino fraction F_G of the lightest neutralino is defined by $F_g = |N_{11}|^2 + |N_{12}|^2$. A gaugino-like LSP may be defined to have F_g very close to 1 ($\gtrsim 0.9$). On the other side, a Higgsino-like LSP would have $F_g \lesssim 0.1$. For values in between, the LSP could be identified as a gaugino-

higgsino mixed state. The MSSM with gaugino masses universal at M_G has a few distinct regions in general that satisfy the WMAP constraint. In this section we point out the existence of such regions in the context of NUSM. i) The *bulk annihilation* region in mSUGRA is typically characterized by smaller scalar masses and smaller values of $m_{1/2}$ where the LSP is bino-dominated. A bino dominated LSP couples favorably with right handed sleptons. Thus, the LSP pair annihilation in the bulk annihilation region occurs primarily via a t-channel sfermion in mSUGRA. There are two important constraints that disfavor the bulk region in mSUGRA. These are the constraints a) from the slepton mass lower limit from LEP2 [46] and b) from the lower limit of Higgs boson mass m_h of 114.4 GeV [47]⁴. ii) The *focus point* [19] or the *Hyperbolic branch* [20] region of mSUGRA is typically characterized by a small $|\mu|$ region that is close to the boundary of lighter chargino mass lower bound. Because of a small $|\mu|$ here the LSP has a significant amount of Higgsino component or it can even be almost a pure Higgsino⁵. Additionally the lighter chargino $\tilde{\chi}_1^\pm$ becomes lighter and coannihilations [43, 44] with LSP reduce the relic density to an acceptable level. The HB/FP region is however absent in NUSM.

iii) Coannihilations of LSP may also occur with sleptons, typically staus ($\tilde{\tau}_1$) [41] in mSUGRA. These regions are associated with small $m_{1/2}$ and small m_0 zones near the boundary of the discarded zone where staus become the LSP. Stau coannihilation is also an effective way to bring the neutralino relic density to an acceptable level in NUSM. Coannihilations of LSP may also occur with stop (\tilde{t}_1) in a general MSSM scenario [42] or even in mSUGRA [48]. However NUSM does not have such region at all.

iv) The most important region satisfying WMAP data for our study is the Higgs-pole annihilation or *funnel* region [49, 50]. The funnel region that satisfies the WMAP data is characterized by the direct-channel pole $2m_{\tilde{\chi}_1^0} \simeq m_A, m_H$. This occurs in mSUGRA typically for large $\tan\beta$ extending to larger m_0 and larger $m_{1/2}$ regions. In NUSM however, the funnel region occurs in all possible $\tan\beta (\gtrsim 5)$. Indeed apart from the LSP-stau coannihilation appearing for a small region, Higgs-pole annihilation is the primary mechanism in NUSM to satisfy the WMAP constraint throughout the parameter space.

We now show the results of the computation of neutralino relic density using the code micrOMEGAs [51]. In Fig.3(a) that corresponds to $\tan\beta = 10$ the region with red dots in

⁴It is quite possible to have a bulk region with a non-zero A_0 [48].

⁵This holds in the inversion region of the Hyperbolic branch [20].

$(m_{\frac{1}{2}} - m_0)$ plane satisfy the WMAP constraint (Eq.15) for the neutralino relic density. For a small m_0 we find the stau coannihilation region marked with red dots. The gray region below the stau coannihilation region is discarded because of appearance of charged LSPs.

The upper gray region is discarded broadly via m_A^2 turning negative except near the boundary where there can be interplay with other constraints as described below. Thus if we concentrate on the boundary of the discarded region the smallest $m_{1/2}$ zone (below 160 GeV or so) is ruled out by the LEP2 lower limit of sparticle masses [46]. This is followed by obtaining tachyonic sfermion scalars (particularly stop scalars) when $m_{\frac{1}{2}}$ is increased further up to $\simeq 600$ GeV. The same boundary zone for the larger $m_{1/2}$ region is eliminated because of the appearance of the charge and color breaking (CCB) minima [52]. In NUSM this happens via the CCB conditions that involve $m_{H_D}^2$, the later becoming negative makes the CCB constraint stronger. In the region between the stau coannihilation area and the upper gray shaded discarded area one finds a long red region that satisfies the WMAP constraint for $\Omega_{\tilde{\chi}_1^0} h^2$. As mentioned before, the reason of satisfying the WMAP data is the direct channel annihilation of two LSPs via neutral Higgs bosons. Fig.3(b) shows a scanned output for $\tan\beta = 10$ when m_0 is varied as in Fig.3(a). The LSP mass is plotted against $(2m_{\tilde{\chi}_1^0} - m_A)/2m_{\tilde{\chi}_1^0}$ so as to show the extent of the A -annihilation or funnel effect. Clearly the WMAP satisfied points shown in red fall around the zero of the y-axis confirming that the funnel region appears in NUSM for small $\tan\beta$ as well. We note that the A -width can be quite large ($\Gamma_A \sim 10$ -50 GeV) and $2m_{\tilde{\chi}_1^0}$ can be several width (Γ_A) away from the exact resonance zone still giving a s -channel annihilation consistent with the WMAP data. The heavy scalar Higgs boson H also significantly contributes to the annihilation cross-section.

We now discuss the result of using a few constraints. First, we use the LEP2 limit [47] of 114.4 GeV for the SM Higgs boson. For the CP-even lighter SUSY Higgs boson mass m_h we use the same constraint as long as we are in the decoupling region [31] where SUSY h -boson is SM-like. In NUSM this is true for almost all the parameter space except a very small region with small $m_{\frac{1}{2}}$ and for $\tan\beta \gtrsim 15$ which we will discuss latter. Additionally, we note that there is an uncertainty of about 3 GeV in computing the mass of light Higgs Boson [53]. This theoretical uncertainty primarily originates from momentum-independent as well as momentum-dependent two-loop corrections, higher loop corrections from top-stop sector etc. Hence, we have drawn a contour for $m_h = 111$ GeV in order to consider an

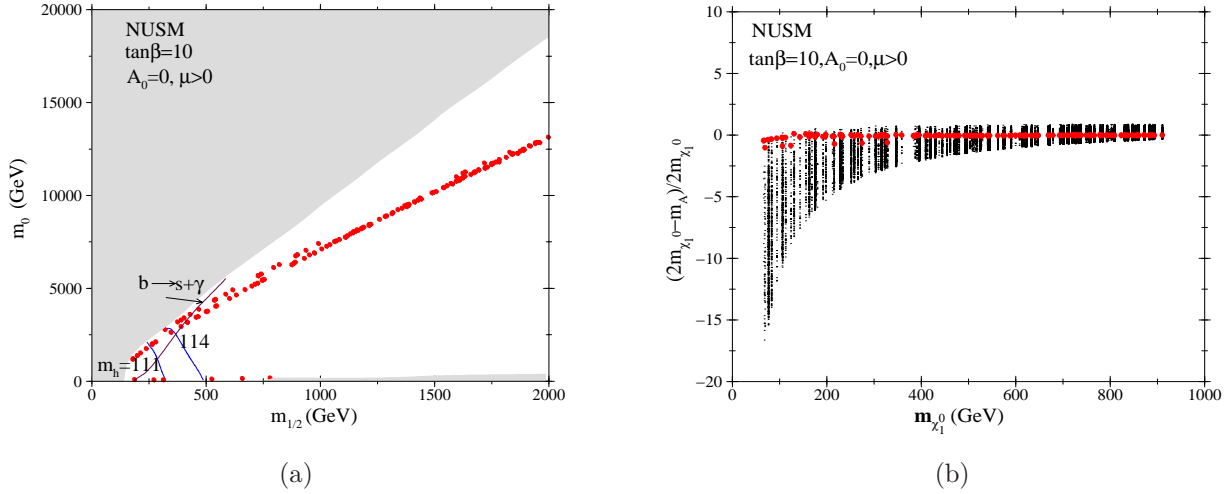


Figure 3: (a) WMAP allowed region in the $m_{1/2} - m_0$ plane for $\tan\beta = 10$ and $A_0 = 0$ with $\mu > 0$ for NUSM. Lighter Higgs boson mass limits are represented by solid lines. Dot-dashed line refers to $b \rightarrow s\gamma$ limit. WMAP allowed regions are shown by red dots. The entire region is allowed via $B_s \rightarrow \mu^+\mu^-$ bound. (b) Scattered points in the plane of $m_{\tilde{\chi}_1^0}$ vs $(2m_{\tilde{\chi}_1^0} - m_A)/2m_{\tilde{\chi}_1^0}$ shown after a scanning of $m_{1/2}$ and m_0 for $\tan\beta = 10$. Almost all the WMAP satisfied points (in red) occur near the zero of the y-axis, thus suggesting the s-channel annihilation of the LSPs via A and H bosons.

effective lower limit.⁶

We have further drawn the $b \rightarrow s\gamma$ contour by considering a 3σ limit [54],

$$2.77 \times 10^{-4} < Br(b \rightarrow s\gamma) < 4.33 \times 10^{-4}. \quad (17)$$

Clearly in Fig.3(a) this constraint would keep $m_{1/2} > 425$ GeV region alive and this is indeed the region of super-large $m_0 \gtrsim 4$ TeV that satisfy the WMAP data. In this context we should however note that $b \rightarrow s + \gamma$ constraint may be of less importance if some additional theoretical assumptions are taken into consideration. Computation of the constraint in models like mSUGRA assumes a perfect alignment of the squark and quark mass-matrices. This essentially considers an unaltered set of mixing angle factors than the Cabibbo-Kobayashi-Maskawa (CKM) factors at the corresponding SM vertices. Even a small set of off-diagonal terms in squark mass matrices at the unification scale may cause a drastic change in the mixing pattern of the squark sector at the electroweak scale. This however does not cause

⁶The following values of top and bottom quarks are considered in the SUSPECT code used in our analysis: $m_t = 172.7$ GeV and $m_b^{\overline{MS}}(m_b) = 4.25$ GeV.

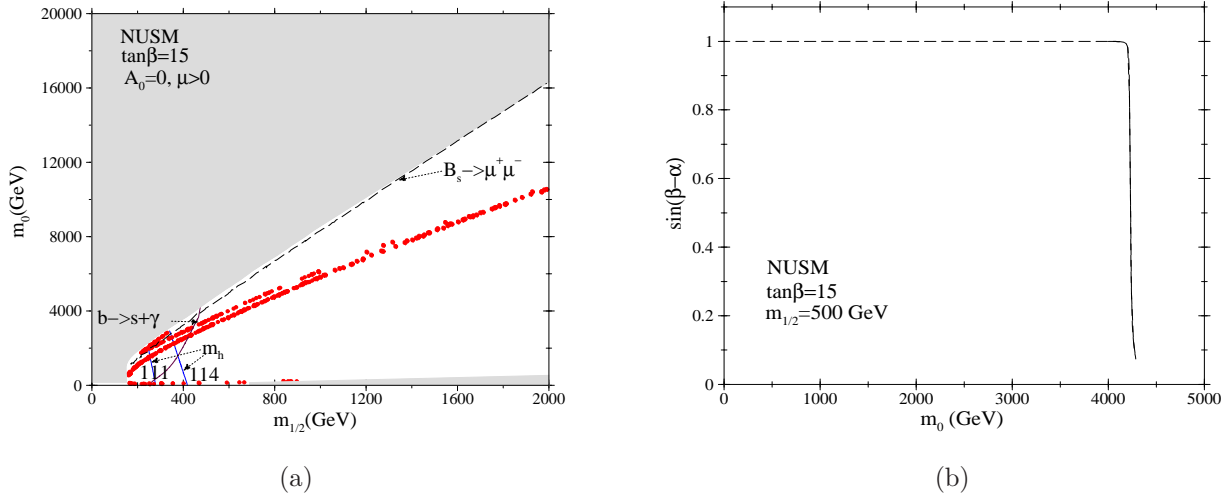


Figure 4: (a) WMAP allowed region in the $m_{1/2} - m_0$ plane for $\tan \beta = 15$ and $A_0 = 0$ with $\mu > 0$ for NUSM. Lighter Higgs boson mass limits are represented by solid lines. Dot-dashed line refers to $b \rightarrow s\gamma$ limit. WMAP allowed regions are shown by red dots. The $B_s \rightarrow \mu^+ \mu^-$ bound is represented by the long-dashed line and this discards a small strip of region below the discarded top gray region. (b) Variation of $\sin(\beta - \alpha)$ vs m_0 for $m_{1/2} = 500$ GeV, $\tan \beta = 15$ and $A_0 = 0$ for NUSM. The figure shows that for large m_0 , actually near the region where m_A is small, $\sin(\beta - \alpha)$ is consistently small. This is of course much away from decoupling region of SUSY Higgs boson.

any effective change in the sparticle mass spectra or in the flavor conserving process of neutralino annihilation or in generating events in a hadron collider in any significant way. A brief review of the model-dependent assumptions for the $b \rightarrow s\gamma$ analyses may be seen in Refs. ([55], [56]) and references therein.

We now explain an interesting aspect of NUSM Higgs boson as a consequence of the LSM effect. As we have seen before, m_A decreases with increasing m_0 in NUSM. We find that with larger m_0 , m_A may become very light for the small $m_{1/2}$ zone so that we may find a spectrum where $m_h \sim m_H \sim M_A$ and this indeed is a consequence of moving into the intense-coupling [32] region of Higgs bosons. This results in a change in the value of the coupling $g_{ZZh} \propto \sin(\beta - \alpha)$, where α is the mixing angle between two neutral Higgs bosons h and H . Typically in the decoupling region $\sin(\beta - \alpha)$ stays very close to 1, but in the intense coupling region this can be considerably small like 0.5 or lesser. This effectively reduces the lower limit of m_h to 93 GeV, a value close to m_Z . In NUSM we obtain this effect for a small region of parameter space (small $m_{1/2}$) if $\tan \beta \gtrsim 15$. Fig.4(a) shows such a region (this

may also satisfy the WMAP limits) for $200 \text{ GeV} \lesssim m_{\frac{1}{2}} \lesssim 300 \text{ GeV}$ and this appears very close to the top gray shaded discarded zone. Fig.4(b) demonstrates the existence of a small $\sin(\beta - \alpha)$ in NUSM as discussed above. However, we will see that such a very light m_A of m_h region with $A_0 = 0$ is almost discarded via the present limit of $B_s \rightarrow \mu^+ \mu^-$. The current experimental limit for $Br(B_s \rightarrow \mu^+ \mu^-)$ coming from CDF [57] puts a strong constraint on the MSSM parameter space. The experimental bound is given by (at 95 % C.L.)

$$\text{Br}(B_s \rightarrow \mu^+ \mu^-) < 5.8 \times 10^{-8} \quad (18)$$

The estimate of $B_s \rightarrow \mu^+ \mu^-$ [58] in MSSM sensitively depends on the mass of A-boson ($\propto m_A^{-4}$) and on the value of $\tan \beta$ ($\propto \tan^6 \beta$). $B_s \rightarrow \mu^+ \mu^-$ constraint eliminates the thin region along the boundary of the REWSB in NUSM where m_A is very light. As mentioned before, for $\tan \beta \gtrsim 15$ a part of the above region for small $m_{\frac{1}{2}}$ zone has non-Standard Model like h -boson.

Apart from the above constraints we would like to remind that there is no non-universality in the first two-generations in NUSM. This saves from the stringent FCNC violating limits such as those coming from the K_L - K_S mass difference or from the $\mu \rightarrow e\gamma$ bound. Splitting of the first generation and the third generation of scalars may also cause violations of FCNC bounds, although to a lesser extent. Data of splitting is important in this regard. Following Ref. [22] we see that for no violation of FCNC one would need (for equal gluino and average squark masses) $|m_{\tilde{q}}(1) - m_{\tilde{q}}(3)| \lesssim m_{\tilde{q}}^2/M_W$. Here $m_{\tilde{q}}$ refers to the average squark mass. Following the analysis performed in Ref. [22] for different gluino masses we conclude that our analysis stays in the safe zone regarding the FCNC bounds in spite of the inter-generational splitting between the squarks.

Fig.5(a) shows similar results for $\tan \beta = 40$. Here the funnel region is extended up to $m_{1/2} = 1.7 \text{ TeV}$. A large value of $\tan \beta$ increases h_b and h_τ and this would enhance the width Γ_A [59]. We point out that unlike Fig.3(a) here the reach of m_0 decreases for a given $m_{1/2}$. The mass of A-boson decreases with increase of m_0 much more rapidly because of larger h_b and h_τ that is associated with a larger $\tan \beta$. Here, the very light m_A region that satisfies the WMAP data and that evades the LEP2 Higgs boson limit exists near the top gray boundary for $250 \text{ GeV} \lesssim m_{\frac{1}{2}} \lesssim 350 \text{ GeV}$ which is again ruled out via the $B_s \rightarrow \mu^+ \mu^-$ limit. The upper gray region is typically discarded here via the REWSB constraint of m_A^2 that turns negative at the tree level. Finally, we have not imposed any limit from the muon $g - 2$ data that may or may not show a discrepancy from the Standard Model result. It is

known that using the recent e^+e^- data leads to a 3.4σ level of discrepancy. On the other hand, using hadronic τ -decay data in computing the leading order hadronic contribution to muon $g - 2$ washes away [60] any deviation from the SM result.

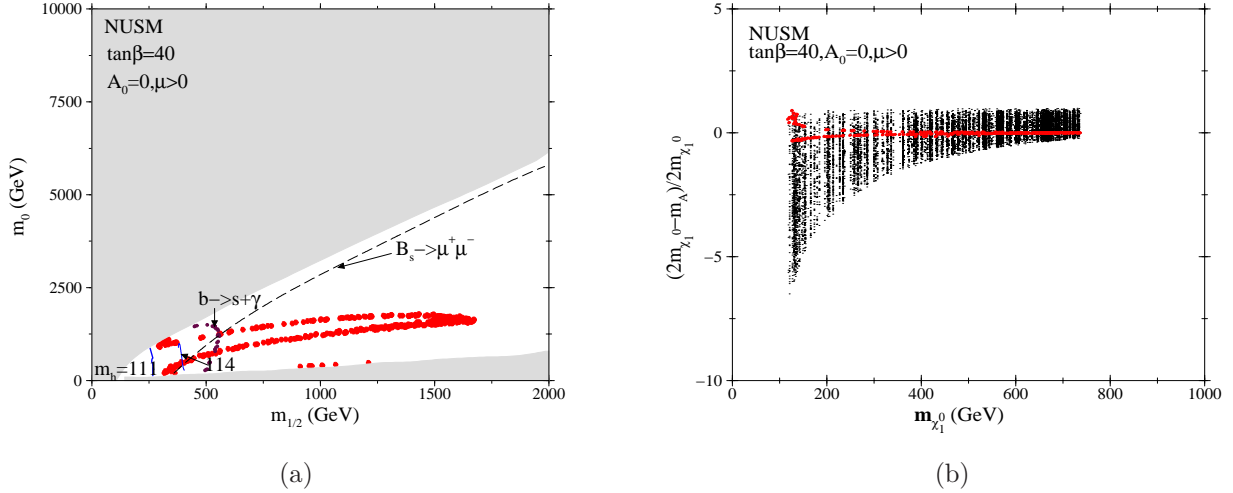


Figure 5: Same as Fig.3 except $\tan\beta = 40$.

3.1 Sample parameter points satisfying WMAP data for early run of LHC

We would focus on a few characteristic parameter points to discuss the nature of the NUSM spectra that satisfies the WMAP limits. Clearly one is able to reach a considerably large m_0 satisfying dark matter relic density constraints and all other necessary constraints for $m_{\frac{1}{2}} < 1$ TeV. As an example with $m_{\frac{1}{2}} = 1$ TeV, this limit is around 7 TeV for $\tan\beta = 10$, 6 TeV for $\tan\beta = 15$, and 1.6 TeV for $\tan\beta = 40$. Thus, for larger $\tan\beta$ the reach of m_0 decreases considerably. On the other hand, it is not unusual to obtain a A -pole annihilation region for a large $\tan\beta$ in popular models like mSUGRA. Hence, if we are interested to focus on a region of MSSM that is not available in mSUGRA type of models we would rather explore the smaller $\tan\beta$ domain of NUSM. The other important zone of parameter space could be the region with smaller $m_{\frac{1}{2}}$ because this would be easily accessible in LHC in its early run. We pick up a point on Fig.3(a) (*scenario-A*) that just satisfies the minimum value of $m_h = 111$ GeV besides being consistent with the WMAP data for cold dark matter. The input parameters are: $\tan\beta = 10$, $A_0 = 0$, $m_{\frac{1}{2}} = 270$ GeV, $m_0 = 2050$ GeV and $sign(\mu) = 1$. The scenario-A of Table 1 thus has light stop and light sbottom quarks, light charginos

and neutralinos and at the same time it would have a light Higgs spectra, all of which are promising for an early LHC detection. We remind ourselves that typically NUSM is associated with a heavy first two-generation of scalars and heavy sleptons for all the three generations. We note that we have relaxed the $b \rightarrow s\gamma$ constraint keeping in mind of the argument given after Eq.17. We could of course respect the constraint, only at a price of having a little heavier spectra, still that would be very much accessible in LHC for the third generation of squarks, Higgs bosons, charginos etc. This however would not cause any essential change in the general pattern. On the other hand, with not so light m_A and with a small $\tan\beta$ the scenario-A satisfies the $B_s \rightarrow \mu^+\mu^-$ limit. The *scenario-B* of Fig.4(a) refers to a special point ($\tan\beta = 15, A_0 = 0, m_{\frac{1}{2}} = 255$ GeV, $m_0 = 2000$ GeV and $\text{sign}(\mu) = 1$) for which the Higgs sector is not in the decoupling region thus reducing the limit of m_h to a value near the Z-boson mass. This parameter point obeys the $B_s \rightarrow \mu^+\mu^-$ limit but as with the *scenario-A* it has an inadequate $Br(b \rightarrow s\gamma)$. With smaller $m_{\frac{1}{2}}$ and smaller m_0 *scenario-B* has a lighter spectrum in general than *scenario-A*. Particularly, we find a much smaller Higgs boson spectra. The *scenario-C* (with $\tan\beta = 40, A_0 = 0, m_{\frac{1}{2}} = 540$ GeV, $m_0 = 1250$ GeV and $\text{sign}(\mu) = 1$), that satisfy all the constraints including the $b \rightarrow s\gamma$ bound provides with a relatively heavier spectra. This is however still within the LHC reach for the relevant part of NUSM as mentioned above. We note that the large m_0 domain of NUSM is typically associated with lighter Higgs spectrum and this region may in general be probed via the production of all MSSM Higgs bosons and subsequently their decays. The squarks corresponding to the first two generations and sleptons of all the generations are large when m_0 is large. As a result the production cross-section of these particles will be too low at the LHC. Thus, to see any SUSY signal for NUSM one should primarily analyze productions and decays of gluino, stop and sbottom in addition to charginos and neutralinos. In a part of the parameter space where the Higgs spectra is light, all the Higgs states may be produced via $pp \rightarrow h, H, A, H^\pm + X$ either via loop-induced processes like ($gg \rightarrow h, H, A$) or through cascade decays via heavier charginos and neutralinos $pp \rightarrow \chi_2^\pm, \chi_3^0, \chi_4^0 \rightarrow \chi_1^\pm, \chi_2^0, \chi_1^0 + h, H, A, H^\pm$. The latter decays are only allowed if enough phase space is available.

parameter	A	B	C
$\tan \beta$	10.0	15.0	40.0
$m_{1/2}$	270.0	255.0	540.0
m_0	2050.0	2000.0	1250.0
A_0	0	0	0
$sgn(\mu)$	1	1	1
μ	312.60	291.53	651.60
$m_{\tilde{g}}$	709.32	674.43	1278.26
$m_{\tilde{u}_L}$	2103.25	2047.68	1658.64
$m_{\tilde{t}_1}$	276.89	248.27	842.00
$m_{\tilde{t}_2}$	493.53	465.21	1028.15
$m_{\tilde{b}_1}$	390.66	354.64	958.59
$m_{\tilde{b}_2}$	434.06	403.08	1019.74
$m_{\tilde{e}_L}$	2050.19	1999.70	1296.33
$m_{\tilde{\tau}_1}$	2037.46	1972.60	1119.32
$m_{\tilde{\chi}_1^\pm}$	196.44	183.99	430.22
$m_{\tilde{\chi}_2^\pm}$	347.34	327.11	668.46
$m_{\tilde{\chi}_4^0}$	347.72	326.97	668.18
$m_{\tilde{\chi}_3^0}$	318.11	297.66	655.13
$m_{\tilde{\chi}_2^0}$	197.69	185.15	430.30
$m_{\tilde{\chi}_1^0}$	108.05	101.72	226.91
m_A	259.48	148.37	403.03
m_{H^+}	272.027	169.44	411.73
m_h	111.26	111.25	116.32
$\Omega_{\tilde{Z}_1} h^2$	0.105	0.102	0.13
$BF(b \rightarrow s\gamma)$	1.59×10^{-4}	4.65×10^{-5}	2.73×10^{-4}
$BF(B_s \rightarrow \mu^+\mu^-)$	4.02×10^{-9}	2.81×10^{-8}	5.29×10^{-8}
Δa_μ	9.31×10^{-11}	1.59×10^{-10}	6.99×10^{-10}

Table 1: Data for point A, B, and C. Masses are in GeV

4 Direct and Indirect detections of dark matter

We will now discuss the prospects of direct and indirect detections [61] of neutralino as a candidate for dark matter in NUSM. First we will discuss the direct detection of LSP via

measurements of nuclear recoil. Neutralinos interact via spin-independent(scalar) and spin-dependent interaction [38,62] with nucleons. The scalar cross-section may be expressed in terms of number of protons and neutrons, Z and $(A - Z)$ respectively [38] as follows.

$$\sigma_{scalar} = 4 \frac{m_r^2}{\pi} [Z f_p + (A - Z) f_n]^2, \quad (19)$$

where m_r is the reduced LSP mass. The quantities f_p and f_n contain all the information of short distance physics and nuclear partonic strengths and these may be seen in Refs. [63]. We will now comment on the relative strengths of spin-independent and spin-dependent neutralino-nuclear cross-sections. While σ_{scalar} depends on Z and $A - Z$ quadratically, the spin-dependent interaction cross-section on the other hand is proportional to $J(J + 1)$ where J is the total nuclear spin [38]. Typically the spin-independent neutralino-nucleon scattering cross-sections (where $\sigma_{\chi p, SI} \simeq \sigma_{\chi n, SI}$) are appreciably smaller than the corresponding spin-dependent cross-sections ($\sigma_{\chi p, SD} \simeq \sigma_{\chi n, SD}$). However considering the fact that $\sigma_{SD} \propto J(J + 1)$ and $\sigma_{SI} \propto Z^2, (A - Z)^2$, σ_{scalar} becomes considerably larger for moderately heavy elements ($A > 30$) [3, 64] like Ge, Xe etc. But we should keep in mind that there exists some cases where σ_{SD} may become considerably larger than σ_{SI} even for $A > 30$.

The cross-section σ_{scalar} mainly involves computation of $\chi - q$ and $\chi - \tilde{g}$ scattering amplitudes. The scalar cross-section at tree level is composed of t -channel Higgs boson exchange and s -channel squark exchange contributions. On the other hand, the spin-dependent cross-section depends on t -channel Z exchange and s -channel squark exchange diagrams. In this analysis we compute the spin-independent cross-section $\sigma_{scalar}(\tilde{\chi} - p)$ for two values of $\tan \beta$ (10 and 40) for $A_0 = 0$ and $\mu > 0$ using DARKSUSY [65]. Fig. (6) shows $\sigma_{scalar}(\tilde{\chi} - p)$ vs $m_{\tilde{\chi}_1^0}$ for $\tan \beta = 10$ and 40 when $m_{1/2}$ and m_0 are varied as in Fig.3 and Fig.5 respectively. The WMAP satisfied points are shown in small (maroon) circles. We have shown the limits from CDMS (Ge) 2005 [66], XENON-10 [67] and future SuperCDMS (Snolab) [68] and XENON1T [69] experiments. The neutralinos with higher mass (< 400 GeV) will be partially probed in XENON-1T while the light LSP region for $\tan \beta = 40$ is already ruled out by XENON-10 data.

The fact that the A-resonance annihilation is the primary mechanism to satisfy the WMAP limits in NUSM suggests that there will be enhanced signals for indirect detection via γ -rays, positrons and anti-protons in NUSM. On the other hand, detection via neutrino signal [61] would not be interesting in this case where the LSP is almost a bino annihilating via A-resonance in the s-channel [59]. Among the above indirect detection possibilities we will

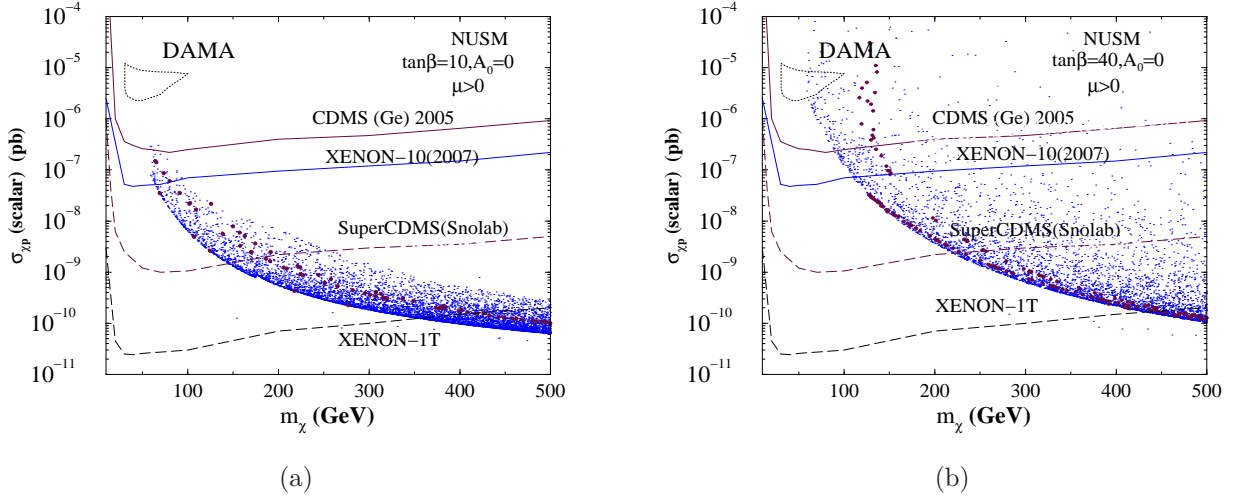


Figure 6: Spin-independent scattering LSP-nucleon cross-sections vs LSP mass for NUSM for $\tan\beta = 10$ and 40 . The blue dotted region correspond to scanned points of the parameter space of Figs.3 and 5. The maroon filled circles show the WMAP allowed points. Various limit plots are shown for different experiments.

limit ourselves with estimating only the detection prospect of gamma rays that originates from the galactic center [70–73]. In general for neutralino annihilation at the galactic center one may have the following possibilities: i) monochromatic γ -rays and ii) continuum γ -rays. Monochromatic γ -rays come out from processes like $\chi\chi \rightarrow \gamma\gamma$ [74] and $\chi\chi \rightarrow Z\gamma$ [75]. These signals although small because of the processes being loop suppressed are clean with definite energies $E_\gamma = m_\chi$ and $E_\gamma = m_\chi - m_Z^2/4m_\chi$. Continuum γ -rays on the other hand arise from neutralinos annihilating into a varieties of Standard Model particles. Hadronization and production of neutral pions would follow. Typically pion decay, in particular $\pi^0 \rightarrow \gamma\gamma$ would produce a huge number of photons with varying energies.

The differential continuum γ -ray flux that arrives from angular direction ψ with respect to the galactic center is given by [61, 71, 72],

$$\frac{d\Phi_\gamma}{dE_\gamma}(E_\gamma, \psi) = \sum_i \frac{\langle \sigma_i v \rangle}{8\pi m_\chi^2} \frac{dN_\gamma^i}{dE_\gamma} \int_{line\ of\ sight} ds \rho_\chi^2(r(s, \psi)) \quad (20)$$

Here σ_i is a LSP pair annihilation cross section into a final channel i . We will consider γ -rays emerging from the galactic center, hence $\psi = 0$. v is the pair's relative velocity and $\langle \sigma v \rangle$ refers to velocity averaged value of σv . $\frac{dN_\gamma^i}{dE_\gamma}$ is the differential γ -ray yield for the channel i . $\rho_\chi(r)$ is the cold dark matter density at a distance r from the galactic center, where $r^2 = s^2 + R_0^2 - 2sR_0 \cos\psi$. Here s is the line of sight coordinate, R_0 is the Solar

distance to the galactic center. Clearly, $\rho_\chi(r)$ that depends on astrophysical modelling is important to determine the photon flux in Eq. (20). One may indeed preferably isolate the right hand side of Eq. (20) into a part depending on particle physics and a part depending on astrophysics. For the later one defines a dimensionless quantity $J(\psi)$ such that,

$$J(\psi) = \left(\frac{1}{8.5 \text{ kpc}} \right) \left(\frac{1}{0.3 \text{ GeV/cm}^3} \right)^2 \int_{\text{line of sight}} ds \rho_\chi^2(r(s, \psi)). \quad (21)$$

The above results into,

$$\frac{d\Phi_\gamma}{dE_\gamma}(E_\gamma, \psi) = 0.94 \times 10^{-13} \text{ cm}^{-2} \text{ s}^{-1} \text{ GeV}^{-1} \text{ sr}^{-1} \sum_i \frac{dN_\gamma^i}{dE_\gamma} \left(\frac{\langle \sigma_i v \rangle}{10^{-29} \text{ cm}^3 \text{ s}^{-1}} \right) \left(\frac{100 \text{ GeV}}{m_\chi} \right)^2 J(\psi) \quad (22)$$

With a detector that has an angular acceptance $\Delta\Omega$ and lowest energy threshold of E_{th} the total gamma ray flux from the galactic center is given by,

$$\Phi_\gamma(E_{th}) = 0.94 \times 10^{-13} \text{ cm}^{-2} \text{ s}^{-1} \sum_i \int_{E_{th}}^{m_\chi} dE_\gamma \frac{dN_\gamma^i}{dE_\gamma} \left(\frac{\langle \sigma_i v \rangle}{10^{-29} \text{ cm}^3 \text{ s}^{-1}} \right) \left(\frac{100 \text{ GeV}}{m_\chi} \right)^2 \bar{J}(\Delta\Omega) \Delta\Omega. \quad (23)$$

Here $\bar{J}(\Delta\Omega) = \frac{1}{\Delta\Omega} \int_{\Delta\Omega} J(\psi) d\Omega$. The upper limit of the integral in Eq.(23) is fixed by the fact that the neutralinos move with galactic velocity therefore the annihilations may be considered to have occurred at rest. We will now comment on the galactic halo density profiles used in this analysis. Various N-body simulations suggests that one may obtain a general profile behavior arbitrary to the extent of a few parameters and this is given by [76],

$$\rho(r) = \rho_0 \frac{[1 + (R_0/a)^\alpha]^{\frac{(\beta-\gamma)}{\alpha}}}{(r/R_0)^\gamma [1 + (r/a)^\alpha]^{\frac{(\beta-\gamma)}{\alpha}}} \quad (24)$$

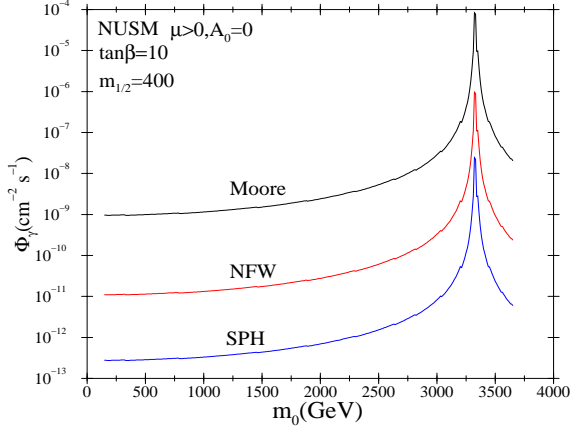
Here ρ_0 is a normalisation factor which taken as the local (*i.e.* solar region) halo density ($\simeq 0.3 \text{ GeV/cm}^3$). We will analyze with three popularly used profiles namely, the isothermal cored [77], Navarro, Frenk and White (NFW) profile [78] and Moore profile [79] as given in the Table (2). The table also mentions the corresponding value of \bar{J} for $\Delta\Omega = 10^{-3}$ and 10^{-5} sr. Computation of photon flux for a different halo profile may easily be performed by an appropriate scaling with the corresponding \bar{J} . Clearly, more cuspy profiles would produce higher photon-flux. One can further include the effects of baryons on the dark matter halo profiles. Baryons may undergo radiative processes leading to a fall towards the central region of a galaxy in formation. This changes the density profiles of matter towards the center which

Halo Model	a (kpc)	R_0 (kpc)	α	β	γ	$\bar{J}(10^{-3})$	$\bar{J}(10^{-5})$
Isothermal cored	3.5	8.5	2	2	0	30.35	30.4
NFW	20.0	8.0	1	3	1	1.21×10^3	1.26×10^4
Moore	28.0	8.0	1.5	3	1.5	1.05×10^5	9.75×10^6

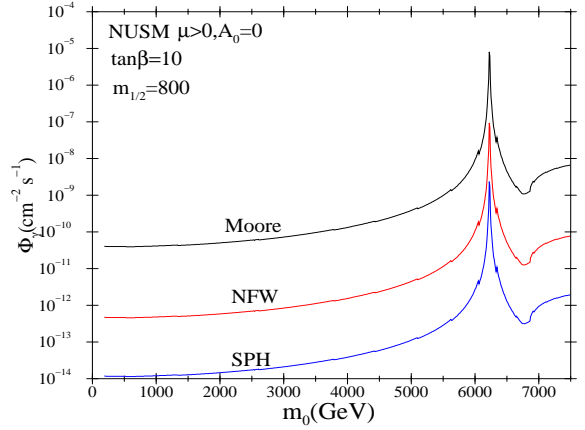
Table 2: A few dark matter halo density profiles and associated parameters.

in turn leads to an increased concentration of dark matter. Adiabatic compression [80] has been used to study the baryonic effects. Inclusion of adiabatic compression effects cause the profiles to become significantly more cuspier, often increasing \bar{J} by a factor of 100 or so [72]. We have not included these halo profile models in our computation, but the photon flux would increase by a similar factor as mentioned above.

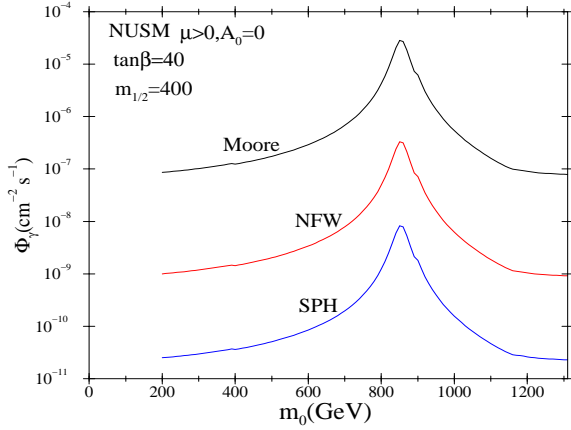
Fig.(7) shows the continuum photon-flux *vs* m_0 results for $\tan\beta = 10$ and 40 corresponding to two different values of $m_{1/2}$ ($= 400$ and 800 GeV) and three different halo profiles as mentioned. The photon flux (in $\text{cm}^{-2}\text{s}^{-1}$) in NUSM is computed using DARKSUSY [65] with $E_\gamma > 1$ GeV for a solid angle aperture of $\Delta\Omega = 10^{-3}$ sr. As m_0 increases the mass of pseudoscalar Higgs boson decreases and the LSP pair annihilation through s-channel resonance causes a peak corresponding to a halo profile. Broadly, such a peak covers the region of m_0 for a given $m_{1/2}$ where WMAP data for neutralino relic density is satisfied. With an increase in $\tan\beta$ the width Γ_A of m_A increases and the peak of a given halo profile curve broadens. We see that in spite of having a broad range of halo profile properties, the photon flux in the region of resonance annihilation in NUSM where the WMAP data is satisfied can be probed in the upcoming GLAST [81, 82] experiment at least for the cuspier profiles. GLAST would be able to probe photon-flux as low as 10^{-10} photons/cm²/s [82]. We note that this conclusion remains valid in spite of the fact that GLAST will use an aperture of $\Delta\Omega = 10^{-5}$ sr so that an appropriate scaling of the photon-flux in Fig.(7) needs to be done from Table (2) and Eq.(23). We further note that as mentioned before, the use of adiabatic compression mechanism would modify a given halo profile significantly and this may increase the photon flux by a few order of magnitude. Fig.(8) shows the plots of photon-flux (in $\text{cm}^{-2}\text{s}^{-1}$ with $E_\gamma > 1$ GeV) vs the mass of LSP for $\tan\beta = 10$ and 40 for a NFW halo profile in NUSM. Here $m_{1/2}$ and m_0 are varied such that $m_{1/2} < 2$ TeV and



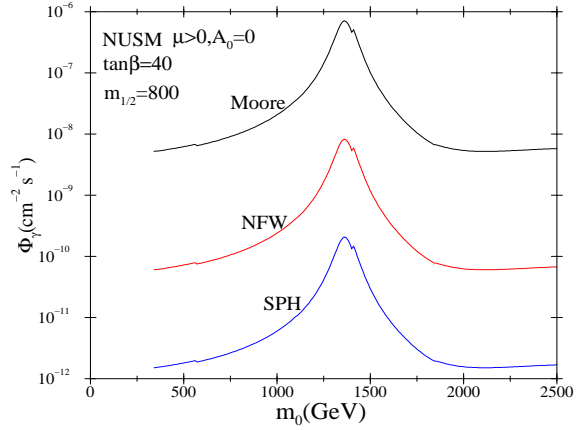
(a)



(b)



(c)



(d)

Figure 7: Continuous γ -ray flux in $\text{cm}^{-2}\text{s}^{-1}$ above a threshold energy of 1 GeV for a cone of 1×10^{-3} sr centered around the galactic center *vs* m_0 . Lines are shown for three different halo distributions i) spherically symmetric isothermal cored profile (SPH) [77], ii) Navarro, Frenk and White (NFW) profile [78] and iii) Moore profile [79].

$m_0 < 20$ TeV for $\tan \beta = 10$ and for $m_{1/2} < 2$ TeV and $m_0 < 10$ TeV for $\tan \beta = 40$. Only WMAP allowed parameter points are shown. GLAST would be able to probe up to 400 to 450 GeV.

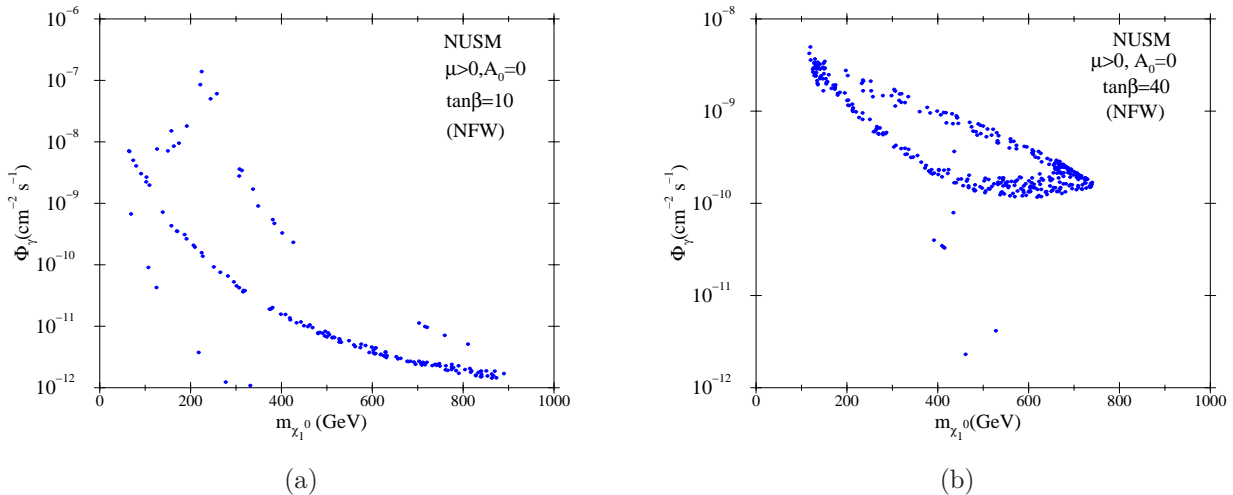


Figure 8: Scatter plot of photon flux in $\text{cm}^{-2}\text{s}^{-1}$ (with $E_\gamma > 1 \text{ GeV}$) vs LSP mass for $\tan\beta = 10$ and 40 for a NFW halo profile in NUSM. Here $m_{1/2}$ and m_0 are scanned in the ranges shown in Figs.(3,5). Only WMAP relic density satisfied points shown.

5 Conclusion

In this analysis we have worked with a non-universal scalar mass scenario of supergravity type of models. We started with purely phenomenological motivations namely, i) to manage FCNC and CP-violation type of constraints by decoupling, ii) to obtain WMAP satisfied values for neutralino relic density for a broad region of parameter space without depending on any delicate mixing of gauginos and Higgsinos, iii) to have radiative electroweak symmetry breaking and iv) to keep naturalness within control. Keeping the above in mind and considering a unified gaugino mass scenario, we used a common scalar mass parameter m_0 at the gauge coupling unification scale for the first two-generation of scalars as well as the third generation of sleptons. The item (i) mentioned above would require m_0 to be large, and the item (iv) would prefer light third generation of squarks and light Higgs scalars. For simplicity we used vanishing third generation of squarks and Higgs scalar masses at the unification scale. In such a scenario with a possibly multi-TeV m_0 , we first found a large mass effect or in particular large slepton mass effect in the RGE of $m_{H_D}^2$ (*ie.* for the down type of Higgs scalar) that turns the later negative at the electroweak scale almost irrespective of a value of $\tan\beta$. Extending the semi-analytic solution of m_A^2 by considering the h_b and the h_τ terms (this is required here even for a small $\tan\beta$) relevant for the large slepton mass effect we found a hyperbolic branch/focus point like effect in $m_A^2 (\simeq m_{H_D}^2 - m_{H_U}^2)$ for small

$\tan\beta$. This causes m_A to be almost independent of m_0 for a large domain of the later. But, with a very large m_0 this causes m_A to become very light or this may even turn m_A^2 negative giving rise to no radiative electroweak symmetry breaking. We further found that because of such large slepton mass effect in the RGE, the Higgs sector may reach an intense coupling region with all the Higgs scalars becoming very light and this may evade the LEP2 limit of m_h for a limited region of parameter space. However, constraint from $Br(B_s \rightarrow \mu^+\mu^-)$ becomes stringent in this region because of lighter m_A . In general, we find relatively lighter m_A or m_H and this fact leads to a large A -pole annihilation region or funnel region of dark matter even for a small $\tan\beta$. This is in contrast to minimal supergravity type of scenarios where funnel region may occur only for large values of $\tan\beta$. The nature of the LSP is bino-dominated, thus there is no need of any delicate mixing of binos and Higgsinos in order to satisfy the neutralino relic density constraint. We have also computed the direct detection rates of LSP-nucleon scattering. The upcoming detectors like XENON-1T would be able to probe almost the entire region of parameter space. We have further estimated the indirect detection prospect via computing continuous photon fluxes. The ongoing GLAST experiment will be successfully able to probe the parameter space even for a less cuspy halo profile. We have also briefly discussed the detection prospect of sparticles in the LHC. The Higgs bosons and the third generation of squarks are light in this scenario. In addition to charginos and neutralinos the above may be easily probed in the early runs of LHC.

6 Appendix

The coefficients appearing in Eqs. 7 and 8 are given by, $C_2 = \frac{\tan^2\beta}{(\tan^2\beta-1)}k$, $C_3 = -\frac{1}{(\tan^2\beta-1)}(g - e \tan^2\beta)$, $C_4 = -\frac{\tan^2\beta}{(\tan^2\beta-1)}f$, $D_2 = \frac{\tan^2\beta+1}{\tan^2\beta-1}k$, $D_3 = -\frac{\tan^2\beta+1}{\tan^2\beta-1}(g-e)$ and $D_4 = -\frac{\tan^2\beta+1}{\tan^2\beta-1}f$. Here the functions k, g, e and f may be seen in Ref. [35]. Electroweak scale result of $Y_i = h_i^2/(4\pi)^2$ with $i \equiv t, b$, and τ are shown below.

$$Y_1(t) = \frac{E_1(t)Y_1(0)}{1 + 6Y_1(0)F(t)}, \quad Y_2(t) = \frac{E_2(t)Y_2(0)}{(1 + 6Y_1(0)F(t))^{\frac{1}{6}}}, \quad \text{and } Y_3(t) = Y_3(0)E_3(t) \quad (25)$$

The quantities $E_i(t)$ are defined as follows.

$$\begin{aligned} E_1(t) &= (1 + \beta_3(t))^{\frac{16}{3b_3}} (1 + \beta_2(t))^{\frac{3}{b_2}} (1 + \beta_1(t))^{\frac{13}{9b_1}} \\ E_2(t) &= (1 + \beta_1(t))^{\frac{-2}{3b_1}} E_1(t) \\ E_3(t) &= (1 + \beta_1(t))^{\frac{3}{b_1}} (1 + \beta_2(t))^{\frac{3}{b_2}} \end{aligned} \quad (26)$$

Here, $F(t) = \int_0^t E_1(t') dt'$, $\beta_i = \alpha_i(0)b_i/4\pi$ and $(b_1, b_2, b_3) = (33/5, 1, -3)$.

Acknowledgments

DD would like to thank the Council of Scientific and Industrial Research, Govt. of India for the support received as a Junior Research Fellow. UC is thankful to the organisers of the workshop “TeV Scale and Dark Matter (2008)” at NORDITA where the last part of the work was completed. UC acknowledges useful discussions with M. Guchait, A. Kundu, B. Mukhopadhyaya, D. Choudhury, D.P. Roy, Jan Kalinowski and S. Roy.

References

- [1] For reviews on Supersymmetry, see, *eg*, H. P. Nilles, Phys. Rep. **1**, 110 (1984); H. E. Haber and G. Kane, Phys. Rep. **117**, 75 (1985); J. Wess and J. Bagger, *Supersymmetry and Supergravity*, 2nd ed., (Princeton, 1991); M. Drees, P. Roy and R. M. Godbole, *Theory and Phenomenology of Sparticles*, (World Scientific, Singapore, 2005).
- [2] T. P. Cheng and L. F. Li, *Oxford, UK: Clarendon (1984) 536 P. (Oxford Science Publications)*
- [3] D. J. H. Chung, L. L. Everett, G. L. Kane, S. F. King, J. D. Lykken and L. T. Wang, Phys. Rept. **407**, 1 (2005); S. P. Martin, arXiv:hep-ph/9709356.
- [4] A. H. Chamseddine, R. Arnowitt and P. Nath, Phys. Rev. Lett. **49**, 970 (1982); R. Barbieri, S. Ferrara and C. A. Savoy, Phys. Lett. B **119**, 343 (1982); L. J. Hall, J. Lykken and S. Weinberg, Phys. Rev. D **27**, 2359 (1983); P. Nath, R. Arnowitt and A. H. Chamseddine, Nucl. Phys. B **227**, 121 (1983); N. Ohta, Prog. Theor. Phys. **70**, 542 (1983); For reviews see [1] and P. Nath, R. Arnowitt and A.H. Chamseddine, *Applied N =1 Supergravity* (World Scientific, Singapore, 1984).
- [5] V. Berezhinsky, A. Bottino, J. Ellis, N. Forrenco, G. Mignola, and S. Scopel, Astropart. Phys. **5**:1-26(1996).
- [6] P. Nath and R. Arnowitt, Phys. Rev. D **56**, 2820 (1997)
- [7] D. G. Cerdeno and C. Munoz, JHEP **0410**, 015 (2004) [arXiv:hep-ph/0405057].

- [8] J. Ellis, K. A. Olive and P. Sandick, arXiv:0805.2343 [hep-ph]; J. R. Ellis, K. A. Olive, Y. Santoso and V. C. Spanos, *Phys. Lett. B* **603**, 51 (2004); J. R. Ellis, T. Falk, K. A. Olive and Y. Santoso, *Nucl. Phys. B* **652**, 259 (2003) [arXiv:hep-ph/0210205]; A. De Roeck, J. R. Ellis, F. Gianotti, F. Moortgat, K. A. Olive and L. Pape, *Eur. Phys. J. C* **49**, 1041 (2007) [arXiv:hep-ph/0508198].
- [9] H. Baer, A. Mustafayev, E. K. Park and X. Tata, *JHEP* **0805**, 058 (2008);
H. Baer, A. Mustafayev, E. K. Park, S. Profumo and X. Tata, *JHEP* **0604**, 041 (2006);
S. Bhattacharya, A. Datta and B. Mukhopadhyaya, arXiv:0804.4051 [hep-ph]; S. Bhattacharya, A. Datta and B. Mukhopadhyaya, arXiv:0809.2012 [hep-ph];
- [10] H. Baer, A. Mustafayev, S. Profumo, A. Belyaev and X. Tata, *JHEP* **0507**, 065 (2005);
H. Baer, A. Mustafayev, S. Profumo, A. Belyaev and X. Tata, *Phys. Rev. D* **71**, 095008 (2005).
- [11] U. Chattopadhyay, D. Choudhury and D. Das, *Phys. Rev. D* **72**, 095015 (2005); U. Chattopadhyay and D. P. Roy, *Phys. Rev. D* **68**, 033010 (2003); A. Corsetti and P. Nath, *Phys. Rev. D* **64**, 125010 (2001); U. Chattopadhyay, A. Corsetti and P. Nath, *Phys. Rev. D* **66**, 035003 (2002); U. Chattopadhyay and P. Nath, *Phys. Rev. D* **65**, 075009 (2002); S. Bhattacharya, A. Datta and B. Mukhopadhyaya, *JHEP* **0710**, 080 (2007); S. Bhattacharya, A. Datta and B. Mukhopadhyaya, arXiv:0804.4051 [hep-ph]; K. Huitu, J. Laamanen, P. N. Pandita and S. Roy, *Phys. Rev. D* **72**, 055013 (2005); K. Huitu, R. Kinnunen, J. Laamanen, S. Lehti, S. Roy and T. Salminen, arXiv:0808.3094 [hep-ph]; S. F. King, J. P. Roberts and D. P. Roy, *JHEP* **0710**, 106 (2007) [arXiv:0705.4219 [hep-ph]]; G. Belanger, F. Boudjema, A. Cottrant, A. Pukhov and A. Semenov, *Nucl. Phys. B* **706**, 411 (2005) [arXiv:hep-ph/0407218].
- [12] S. K. Soni and H. A. Weldon, *Phys. Lett.* **B126**, 215(1983); V. S. Kaplunovsky and J. Louis, *Phys. Lett.* **B306**, 268(1993).
- [13] M. Dine, R. Leigh, and A. Kagan, *Phys. Rev.* **D48**, 4269 (1993); P. Pouliot and N. Seiberg, *Phys. Lett.* **B318**, 169 (1993); Y. Nir and N. Seiberg, *Phys. Lett.* **B309**, 337 (1993). S. Dimopoulos and G.F. Giudice, *Phys. Lett.* **B357**, 573 (1995); A. Cohen, D.B. Kaplan, and A.E. Nelson, *Phys. Lett.* **B388**, 588 (1996); M. Misiak, S. Pokorski and

- J. Rosiek, *Adv. Ser. Direct. High Energy Phys.* **15**, 795 (1998) [arXiv:hep-ph/9703442];
P. H. Chankowski, K. Kowalska, S. Lavignac and S. Pokorski, arXiv:hep-ph/0507133.
- [14] N. Arkani-Hamed and H. Murayama, *Phys. Rev. D* **56**, 6733 (1997) [arXiv:hep-ph/9703259].
- [15] F. Gabbiani, E. Gabrielli, A. Masiero and L. Silvestrini, *Nucl. Phys. B* **477**, 321 (1996) [arXiv:hep-ph/9604387].
- [16] R. Barbieri and G.F. Giudice, *Nucl. Phys.* **B306**,63(1988); P. Ciafaloni and A. Strumia, *Nucl. Phys.* **B494**, 41(1997); G. Bhattacharya and A. Romanino, *Phys. Rev.* **D55**, 7015(1997).
- [17] J. Bagger, J. L. Feng and N. Polonsky, *Nucl. Phys. B* **563**, 3 (1999); . K. Agashe and M. Graesser, *Phys. Rev. D* **59**, 015007 (1999); J. A. Bagger, J. L. Feng, N. Polonsky and R. J. Zhang, *Phys. Lett. B* **473**, 264 (2000).
- [18] H. Baer, C. Balazs, P. Mercadante, X. Tata and Y. Wang, *Phys. Rev. D* **63**, 015011 (2001) [arXiv:hep-ph/0008061].
- [19] J. L. Feng, K. T. Matchev and T. Moroi, *Phys. Rev. D* **61**, 075005 (2000); *Phys. Rev. Lett.* **84**, 2322 (2000); J. L. Feng, K. T. Matchev and F. Wilczek, *Phys. Lett. B* **482**, 388 (2000); J. L. Feng and F. Wilczek, *Phys. Lett. B* **631**, 170 (2005); U. Chattopadhyay, T. Ibrahim and D. P. Roy, *Phys. Rev. D* **64**, 013004 (2001); U. Chattopadhyay, A. Datta, A. Datta, A. Datta and D. P. Roy, *Phys. Lett. B* **493**, 127 (2000); S. P. Das, A. Datta, M. Guchait, M. Maity and S. Mukherjee, *Eur. Phys. J. C* **54**, 645 (2008), [arXiv:0708.2048 [hep-ph]].
- [20] K. L. Chan, U. Chattopadhyay and P. Nath, *Phys. Rev. D* **58**, 096004 (1998); [arXiv:hep-ph/9710473]; U. Chattopadhyay, A. Corsetti and P. Nath, *Phys. Rev. D* **68**, 035005 (2003) [arXiv:hep-ph/0303201];
See also: 1st article of Ref. [39].
- [21] V. D. Barger, C. Kao and R. J. Zhang, *Phys. Lett. B* **483**, 184 (2000) [arXiv:hep-ph/9911510].

- [22] H. Baer, A. Belyaev, T. Krupovnickas and A. Mustafayev, JHEP **0406**, 044 (2004) [arXiv:hep-ph/0403214].
- [23] S. F. King and J. P. Roberts, JHEP **0609**, 036 (2006);
- [24] D. G. Cerdeno, S. Khalil and C. Munoz, arXiv:hep-ph/0105180.
- [25] N. Arkani-Hamed, A. Delgado and G. F. Giudice, Nucl. Phys. B **741**, 108 (2006), [arXiv:hep-ph/0601041].
- [26] C. D. McMullen and S. Nandi, Phys. Rev. D **75**, 095001 (2007)
- [27] D. Feldman, Z. Liu and P. Nath, JHEP **0804**, 054 (2008); D. Feldman, Z. Liu and P. Nath, Phys. Rev. Lett. **99**, 251802 (2007) [Erratum-ibid. **100**, 069902 (2008)].
- [28] L. Randall and R. Sundrum, Nucl. Phys. **B557**(1999) 79. G.F. Giudice, M.A. Luty, H. Murayama, and R. Rattazzi, J. High Energy Phys. **12**(1998) 027. T. Gherghetta, G.F. Giudice, and J.D. Wells, Nucl. Phys. **B559** (1999) 27.
- [29] A. Brignole, L. E. Ibanez and C. Munoz, Nucl. Phys. B **422**, 125 (1994) [Erratum-ibid. B **436**, 747 (1995)] L. E. Ibanez, D. Lust and G. G. Ross, Phys. Lett. B **272**, 251 (1991).
- [30] D. G. Cerdeno, T. Kobayashi and C. Munoz, arXiv:0709.0858 [hep-ph].
- [31] H.E. Haber and Y. Nir, Phys. Lett. **B306** 327 (1993); H.E. Haber, hep-ph/9505240; A. Dobado, M.J. Herrero and S. Penaranda, Eur. Phys. J. **C17** 487 (2000) ; J.F. Gunion and H.E. Haber, Phys. Rev. **D67** 075019 (2003).
- [32] A. Djouadi and Y. Mambrini, JHEP **0612**, 001 (2006); E. Boos, V. Bunichev, A. Djouadi and H.J. Schreiber, Phys. Lett. **B622** 311 (2005); E. Boos, A. Djouadi and A. Nikitenko, Phys. Lett. **B578**, 384 (2004); E. Boos, A. Djouadi, M. Muhlleitner and A. Vologdin, Phys. Rev. **D66** 055004 (2002).
- [33] R. Arnowitt and P. Nath, Phys. Rev. D **46**, 3981 (1992).
- [34] G. Gamberini, G. Ridolfi and F. Zwirner, Nucl. Phys. B **331**, 331 (1990); V. D. Barger, M. S. Berger and P. Ohmann, Phys. Rev. D **49**, 4908 (1994); For two-loop effective potential see: S. P. Martin, Phys. Rev. D **66**, 096001 (2002).

- [35] L. E. Ibanez, C. Lopez and C. Munoz, Nucl. Phys. B **256**, 218 (1985); L. E. Ibanez and C. Lopez Nucl. Phys. B **233**, 511 (1984).
- [36] A. Djouadi, J. L. Kneur and G. Moultaka, arXiv:hep-ph/0211331.
- [37] J. R. Ellis, K. A. Olive and P. Sandick, Phys. Lett. B **642**, 389 (2006) [arXiv:hep-ph/0607002].
- [38] G. Jungman, M. Kamionkowski and K. Greist, Phys. Rep. **267**, 195 (1995).
- [39] A. B. Lahanas, N. E. Mavromatos and D. V. Nanopoulos, Int. J. Mod. Phys. D **12**, 1529 (2003) [arXiv:hep-ph/0308251]; C. Munoz, Int. J. Mod. Phys. A **19**, 3093 (2004) [arXiv:hep-ph/0309346]; Manuel Drees, Plenary talk at 11th International Symposium on Particles, Strings and Cosmology (PASCOS 2005), Gyeongju, Korea, 30 May - 4 Jun 2005 (published in AIP Conf.Proc., **805**, 48-54, (2006)).
- [40] E. Komatsu *et al.* [WMAP Collaboration], arXiv:0803.0547 [astro-ph].
- [41] J. R. Ellis, T. Falk and K. A. Olive, Phys. Lett. B **444**, 367 (1998); J. R. Ellis, T. Falk, K. A. Olive and M. Srednicki, Astropart. Phys. **13**, 181 (2000) [Erratum-ibid. **15**, 413 (2001)]; A. Lahanas, D. V. Nanopoulos and V. Spanos, Phys. Rev. D **62**, 023515 (2000); R. Arnowitt, B. Dutta and Y. Santoso, Nucl. Phys. B **606**, 59 (2001); T. Nihei, L. Roszkowski and R. Ruiz de Austri, JHEP **0207**, 024 (2002); V. A. Bednyakov, H. V. Klapdor-Kleingrothaus and V. Gronewold, Phys. Rev. D **66**, 115005 (2002).
- [42] C. Boehm, A. Djouadi and Manuel Drees, Phys. Rev. D **62**, 035012 (2000); J. R. Ellis, K. A. Olive and Y. Santoso, Astropart. Phys. **18**, 395 (2003);
See also Ref. [48].
- [43] J. Edsjo and P. Gondolo, Phys. Rev. D **56**, 1879 (1997).
- [44] S. Mizuta and M. Yamaguchi, Phys. Lett. B **298**, 120 (1993) [arXiv:hep-ph/9208251].
- [45] R. Arnowitt, B. Dutta and Y. Santoso, Nucl. Phys. B **606**, 59 (2001); V. A. Bednyakov, H. V. Klapdor-Kleingrothaus and V. Gronewold, arXiv:hep-ph/0208178.
- [46] For the latest limits on the sparticle masses from LEP experiments: see <http://lepsusy.web.cern.ch/lepsusy/>

- [47] R. Barate *et al.* [LEP Working Group for Higgs boson searches], Phys. Lett. B **565**, 61 (2003) [arXiv:hep-ex/0306033].
- [48] U. Chattopadhyay, D. Das, A. Datta and S. Poddar, Phys. Rev. D **76**, 055008 (2007) [arXiv:0705.0921 [hep-ph]]; N. Bhattacharyya, A. Datta and S. Poddar, arXiv:0807.0278 [hep-ph].
- [49] M. Drees and M. Nojiri, Phys. Rev. **D47**, 376 (1993).
- [50] R. Arnowitt and P. Nath, Phys. Rev. Lett. **70**, 3696 (1993); H. Baer and M. Brhlik, Phys. Rev. **D53**, 597 (1996), Phys. Rev. D **57**, 567 (1998); H. Baer, M. Brhlik, M. Diaz, J. Ferrandis, P. Mercadante, P. Quintana and X. Tata, Phys. Rev. **D63**, 015007 (2001); J. R. Ellis, T. Falk, G. Ganis, K. A. Olive and M. Srednicki, Phys. Lett. B **510**, 236 (2001); A. B. Lahanas and V. C. Spanos, Eur. Phys. J. C **23**, 185 (2002); A. Djouadi, M. Drees and J. Kneur, Phys. Lett. B **624** 60 (2005).
- [51] G. Belanger, F. Boudjema, A. Pukhov and A. Semenov, Comput. Phys. Commun. **176**, 367 (2007) [arXiv:hep-ph/0607059].
- [52] J. M. Frere, D. R. T. Jones and S. Raby, Nucl. Phys. B **222**, 11 (1983); J. A. Casas, A. Lleyda and C. Munoz, Nucl. Phys. B **471**, 3 (1996) [arXiv:hep-ph/9507294].
- [53] S. Heinemeyer, W. Hollik and G. Weiglein, Phys. Rep. **425**, 265 (2006); S. Heinemeyer, hep-ph/0408340; S. Heinemeyer, Int. J. Mod. Phys. A **21**, 2659 (2006); G. Degrassi, S. Heinemeyer, W. Hollik, P. Slavich and G. Weiglein, Eur. Phys. J. C **28**, 133 (2003); B. C. Allanach, A. Djouadi, J. L. Kneur, W. Porod and P. Slavich, JHEP **0409**, 044 (2004).
- [54] S. Chen, *et al.*, CLEO Collaboration, Phys. Rev. Lett. **87**, 251807 (2001), hep-ex/0108032; P. Koppenburg *et al.* [Belle Collaboration], Phys. Rev. Lett. **93**, 061803 (2004) B. Aubert, *et al.*, BaBar Collaboration, hep-ex/0207076.
- [55] K. i. Okumura and L. Roszkowski, Phys. Rev. Lett. **92**, 161801 (2004); M. E. Gomez, T. Ibrahim, P. Nath and S. Skadhauge, Phys. Rev. D **74**, 015015 (2006).
- [56] A. Djouadi, M. Drees and J. L. Kneur, JHEP **0603**, 033 (2006).

- [57] T. Aaltonen *et al.* [CDF Collaboration], Phys. Rev. Lett. **100**, 101802 (2008).
- [58] J.R. Ellis, K.A. Olive and V.C. Spanos, Phys. Lett. B **624**, 47 (2005); T. Ibrahim and P. Nath, Phys. Rev. D **67**, 016005 (2003); S. Baek, P. Ko, and W. Y. Song, JHEP **0303**, 054 (2003); J. K. Mizukoshi, X. Tata and Y. Wang, Phys. Rev. D **66**, 115003 (2002); R. Arnowitt, B. Dutta, T. Kamon and M. Tanaka, Phys. Lett. B **538** (2002) 121; A. Dedes, H. K. Dreiner, U. Nierste, and P. Richardson, Phys. Rev. Lett. **87**, 251804 (2001); K. S. Babu and C. Kolda, Phys. Rev. Lett. **84**, 228 (2000); S. R. Choudhury and N. Gaur, Phys. Lett. B **451**, 86 (1999).
- [59] H. Baer, A. Belyaev, T. Krupovnickas and J. O’Farrill, JCAP **0408**, 005 (2004); H. Baer and J. O’Farrill, JCAP **0404**, 005 (2004).
- [60] M. Passera, W. J. Marciano and A. Sirlin, Phys. Rev. D **78**, 013009 (2008).
- [61] G. Bertone, D. Hooper and J. Silk, Phys. Rept. **405**, 279 (2005); G. Bertone and D. Merritt, Mod. Phys. Lett. A **20**, 1021 (2005); J. Carr, G. Lamanna and J. Lavalle, Rept. Prog. Phys. **69**, 2475 (2006).
- [62] M. W. Goodman and E. Witten, Phys. Rev. D **31**, 3059 (1985); K. Greist, Phys. Rev. **D38**, 2357(1988); J. Ellis and R. Flores, Nucl. Phys. **B307**, 833(1988); R. Barbieri, M. Frigeni and G. Giudice, Nucl. Phys. **B313**, 725(1989); A. Bottino et.al., **B295**, 330(1992); M. Drees and M.M. Nojiri, Phys. Rev.**D48**,3483(1993); J. R. Ellis, A. Ferstl and K. A. Olive, Phys. Lett. B **481**, 304 (2000); J. D. Vergados, Lect. Notes Phys. **720**, 69 (2007); V. K. Oikonomou, J. D. Vergados and C. C. Moustakidis, Nucl. Phys. B **773**, 19 (2007); J. Ellis, K. A. Olive and C. Savage, Phys. Rev. D **77**, 065026 (2008); D. Feldman, Z. Liu and P. Nath, Phys. Lett. B **662**, 190 (2008); D. Feldman, Z. Liu and P. Nath, arXiv:0808.1595 [hep-ph].
- [63] M. Drees and M. Nojiri, Phys. Rev. **D47**, 4226 (1993) and Phys. Rev. **D48**, 3483 (1993); M. A. Shifman, A. I. Vainshtein and V. I. Zakharov, Phys. Lett. **78B**, 443 (1978); A. I. Vainshtein, V. I. Zakharov and M. A. Shifman, Usp. Fiz. Nauk **130**, 537 (1980).
- [64] V. A. Bednyakov, H. V. Klapdor-Kleingrothaus and S. Kovalenko, Phys. Rev. D **50**, 7128 (1994) [arXiv:hep-ph/9401262].

- [65] P. Gondolo, J. Edsjo, P. Ullio, L. Bergstrom, M. Schelke and E. A. Baltz, JCAP **0407**, 008 (2004) [arXiv:astro-ph/0406204].
- [66] D. S. Akerib *et al.* [CDMS Collaboration], Phys. Rev. Lett. **96**, 011302 (2006) [arXiv:astro-ph/0509259]
- [67] J. Angle *et al.* [XENON Collaboration], Phys. Rev. Lett. **100**, 021303 (2008) [arXiv:0706.0039 [astro-ph]].
- [68] http://www.fermilabtoday.com/directorate/program_planning/March2007PACPublic/CabreraPAC03_07.pdf;
For a limit plot see: <http://dendera.berkeley.edu/plotter/entryform.html>
- [69] http://www.lngs.infn.it/lngs_infn/contents/lngs_en/research/experiments_scientific_info/experiments/current/xenon/collaboration.htm;
For a limit plot see : <http://dendera.berkeley.edu/plotter/entryform.html>
- [70] A. Bouquet, P. Salati and J. Silk, Phys. Rev. D **40**, 3168 (1989); F. W. Stecker, Phys. Lett. B **201**, 529 (1988); M. Urban, A. Bouquet, B. Degrange, P. Fleury, J. Kaplan, A. L. Melchior and E. Pare, Phys. Lett. B **293**, 149 (1992); V. S. Berezinsky, A. V. Gurevich and K. P. Zybin, Phys. Lett. B **294**, 221 (1992); V. Berezinsky, A. Bottino and G. Mignola, Phys. Lett. B **325**, 136 (1994); G. Bertone, G. Sigl and J. Silk, Mon. Not. Roy. Astron. Soc. **337**, 98 (2002) [arXiv:astro-ph/0203488]; T. Bringmann, L. Bergstrom and J. Edsjo, JHEP **0801**, 049 (2008).
- [71] L. Bergstrom, P. Ullio and J. H. Buckley, Astropart. Phys. **9**, 137 (1998) [arXiv:astro-ph/9712318].
- [72] Y. Mambrini, C. Munoz, E. Nezri and F. Prada, JCAP **0601**, 010 (2006); Y. Mambrini, C. Munoz and E. Nezri, JCAP **0612**, 003 (2006); L. Roszkowski, R. R. de Austri, J. Silk and R. Trotta, arXiv:0707.0622 [astro-ph]; S. Profumo and A. Provenza, JCAP **0612**, 019 (2006); H. Baer, A. Mustafayev, E. K. Park and S. Profumo, JHEP **0507**, 046 (2005);
- [73] S. Dodelson, D. Hooper and P. D. Serpico, Phys. Rev. D **77**, 063512 (2008); D. Hooper, G. Zaharijas, D. P. Finkbeiner and G. Dobler, Phys. Rev. D **77**, 043511 (2008); D. Hooper and E. A. Baltz, arXiv:0802.0702 [hep-ph]; N. Bernal, A. Goudelis, Y. Mambrini and

- C. Munoz, arXiv:0804.1976 [hep-ph]; A. Birkedal, K. T. Matchev, M. Perelstein and A. Spray, arXiv:hep-ph/0507194;
- [74] L. Bergstrom and P. Ullio, ‘Full one-loop calculation of neutralino annihilation into two photons’, *Nucl. Phys.* **B504**, 27 (1997); Z. Bern P. Gondolo and M. Perelstein, ‘Neutralino annihilation into two photons’, *Phys. Lett.* **B411**, 86 (1997); U. Chattopadhyay, D. Das, P. Konar and D. P. Roy, *Phys. Rev. D* **75**, 073014 (2007); U. Chattopadhyay, D. Choudhury, M. Drees, P. Konar and D. P. Roy, *Phys. Lett. B* **632**, 114 (2006).
- [75] P. Ullio and L. Bergstrom, *Phys. Rev. D* **57**, 1962 (1998) [arXiv:hep-ph/9707333].
- [76] L. Hernquist, *Astrophys. J.* **356**, 359 (1990).
- [77] J. Binney and S. Tremaine, *Galactic Dynamics*, (Princeton University Press, Princeton, 1987).
- [78] J.F. Navarro, C.S. Frenk, S.D.M. White, *Astrophys. J.* 462 (1996) 563; J.F. Navarro, C.S. Frenk, S.D.M. White, *Astrophys. J.* 490 (1997) 493.
- [79] B. Moore, T. Quinn, F. Governato, J. Stadel and G. Lake, *Mon. Not. Roy. Astron. Soc.* **310**, 1147 (1999) [arXiv:astro-ph/9903164].
- [80] G. R. Blumenthal, S. M. Faber, R. Flores and J. R. Primack, *Astrophys. J.* **301**, 27 (1986); R. Jesseit, T. Naab and A. Burkert, *Astrophys. J. Lett* **571**, L89 (2002), arXiv:astro-ph/0204164; O. Y. Gnedin, A. V. Kravtsov, A. A. Klypin and D. Nagai, *Astrophys. J.* **616**, 16 (2004) [arXiv:astro-ph/0406247]; F. Prada, A. Klypin, J. Flix, M. Martinez and E. Simonneau, arXiv:astro-ph/0401512;
- [81] The gamma-ray large area space telescope (GLAST): <http://glast.gsfc.nasa.gov>;
- [82] A. Morselli, A. Lionetto, A. Cesarini, F. Fucito and P. Ullio [GLAST Collaboration], *Nucl. Phys. Proc. Suppl.* **113**, 213 (2002) [arXiv:astro-ph/0211327].